The *ULTRACURVATA2* Gene of Arabidopsis Encodes an FK506-Binding Protein Involved in Auxin and Brassinosteroid Signaling[1]

José Manuel Pérez-Pérez, María Rosa Ponce, and José Luis Micol*

División de Genética and Instituto de Bioingeniería, Universidad Miguel Hernández, Campus de Elche, 03202 Elche, Alicante, Spain

The dwarf *ucu* (*ultracurvata*) mutants of Arabidopsis display vegetative leaves that are spirally rolled downwards and show reduced expansion along the longitudinal axis. We have previously determined that the *UCU1* gene encodes a SHAGGY/ GSK3-like kinase that participates in the signaling pathways of auxins and brassinosteroids. Here, we describe four recessive alleles of the *UCU2* gene, whose homozygotes display helical rotation of several organs in addition to other phenotypic traits shared with *ucu1* mutants. Following a map-based strategy, we identified the *UCU2* gene, which was found to encode a peptidyl-prolyl cis/trans-isomerase of the FK506-binding protein family, whose homologs in metazoans are involved in cell signaling and protein trafficking. Physiological and double mutant analyses suggest that *UCU2* is required for growth and development and participates in auxin and brassinosteroid signaling.

Plant growth and development are ruled by environmental and endogenous signals, which are integrated through genetic networks that finally act on the division, expansion, and differentiation of cells to generate specific developmental patterns (Tsiantis and Langdale, 1998). Brassinosteroids (BRs) are steroid hormones belonging to the group of endogenous signals required for plant growth and organogenesis, controlling processes such as cell expansion, vascular differentiation, etiolation, reproductive development, and stress responses (Bishop and Yokota, 2001; Bishop and Koncz, 2002).

The biosynthetic pathway of brassinolide, the most active BR, has been dissected thanks to the genetic and molecular analysis of Arabidopsis dwarf mutants (Altmann, 1999; Li and Chory, 1999; Bishop and Yokota, 2001). Little is known, however, about the genes involved in BR signal transduction (Altmann, 2001; Friedrichsen and Chory, 2001; Bishop and Koncz, 2002; Clouse, 2002). Among the BR-insensitive dwarf mutants isolated until now, all those carrying recessive mutations were shown to be affected in the *BRI1* (*BRASSINOSTEROID INSENSITIVE1*) gene, which codes for a cell-surface Leu-rich repeat receptor Ser/Thr kinase (Li and Chory, 1997; He et al., 2000; Wang et al., 2001). BRI1 transduces the BR signal into the nucleus through a mostly unknown phosphorylation cascade (Friedrichsen et al., 2000), leading to the differential expression of target genes, some of which are assumed to control cell expansion (Müssig et al., 2002). On the contrary, BR-insensitive semidominant dwarf mutants carry mutations in the *UCU1* (*ULTRACURVATA1*; Berná et al., 1999) gene, also named *BIN2* (*BRASSINO-STEROID INSENSITIVE2*; Li et al., 2001a), which encodes a member of the SHAGGY/GSK3 family of intracellular protein kinases (Li and Nam, 2002; Pérez-Pérez et al., 2002), whose metazoan homologs are involved in the negative regulation of several developmental pathways, such as those of insulin or Wingless/Wnt signaling (Kim and Kimmel, 2000; Cohen and Frame, 2001). More recently, screenings based on the use of a specific BR-biosynthesis inhibitor have led to the identification of dominant mutations in the *BZR1* (*BRASSINAZOLE RESISTANT1*; Wang et al., 2002) gene and its homolog *BES1* (*BRI1-EMS-SUPPRESSOR1*), also named *BZR2* (Yin et al., 2002), the protein products of which are positive regulators of the BR signaling pathway and cooperatively regulate the expression of BR target genes. BIN2 (UCU1) has been shown to be a negative regulator of the BR signaling pathway that destabilizes BZR1 and BES1 by phosphorylation, in an analogous way to that of SHAGGY/GSK3 over β-catenin in the Wingless/Wnt pathway (He et al., 2002; Yin et al., 2002).

In this work, we present the genetic and molecular analyses of four loss-of-function, recessive alleles of the *UCU2* gene, the phenotype of which is extremely similar to that of plants homozygous for the semidominant alleles of the *UCU1* gene, sharing most phenotypic traits such as dwarfism and circinate leaves.

In addition, *ucu2/ucu2* plants display helical rotation of some of their organs. We identified the *UCU2* gene by a map-based approach and found that it encodes an FK506 binding-like protein (FKBP), named At-FKBP42. FKBPs are a class of peptidyl-prolyl cis/trans-isomerases (PPIases) that play critical roles in regulating cellular processes through protein activation (Harrar et al., 2001; Schiene-Fischer and Yu, 2001). The *twd1* (*twisted dwarf1*) mutant, which is phenotypically indistinguishable of the *ucu2* mutants, is also defective in AtFKBP42 (B. Schulz, unpublished data; quoted in Kamphausen et al., 2002), which indicates that *TWD* and *UCU2* are the same gene. The responses of *ucu2* mutants to exogenous plant hormones and the genetic analysis of *ucu2* alleles suggest that *UCU2* participates in auxin and BR signaling.

RESULTS

Isolation of *ultracurvata2* Mutants

In a large-scale screening for Arabidopsis mutants displaying abnormally shaped or sized leaves (Berná et al., 1999; Serrano-Cartagena et al., 1999; Robles and Micol, 2001), one of the strongest leaf phenotypes found was that of *ucu* (*ultracurvata*) mutants, whose vegetative leaves are rolled spirally downwards, in a circinate manner (Fig. 1, B–D). Five *ucu* lines were identified among our mutants, which were found to fall into two complementation groups. On the one hand, the *UCU1* gene was represented by one recessive (Fig. 1B) and two semidominant ethyl methanesulfonate-induced alleles (Fig. 1C; Pérez-Pérez et al., 2002). On the other hand, the *UCU2* complementation group included two recessive alleles, *ucu2-1* (Fig. 1D) and *ucu2-3*, which were respectively induced by fast neutron bombardment (P. Robles and J.L. Micol, unpublished data) and T-DNA insertional mutagenesis (this work). Although it was isolated from a collection of lines carrying T-DNA insertions, we found the *ucu2-3* mutation to be untagged (data not shown). Another line displaying the Ultracurvata phenotype, CS3397, initially named *inl* (*invalida*) by Rédei, was obtained from the ABRC and found to be a double mutant carrying the *ucu2-2* and *gi-2* (*gigantea-2*; Rédei, 1962) recessive mutations, the latter conferring an extremely late flowering phenotype, both of them putatively induced by x-ray mutagenesis. After backcrossing the CS3397 line to Columbia-0 (Col-0), F_2 plants that displayed the Ultracurvata phenotype and normal flowering time were isolated, and the absence of the *gi-2* mutation was confirmed in their F_3 progeny.

Figure 1. The Ultracurvata phenotype. A to D, Rosettes from a Landsberg *erecta* (L*er*) wild-type individual (A) and several *ucu* mutants: B, *ucu1-3/ucu1-3*; C, *ucu1-2/ucu1-2*; and D, *ucu2-1/ucu2-1*. Vegetative (E, third node) and cauline (F, eighth node) leaves from an *ucu2-1/ucu2-1* individual. G and H, Inflorescence of *ucu2-1/ucu2-1* (G) and *ucu2-3/ucu2-3* (H) plants. I and J, Helical rotation in some organs of *ucu2-1/ucu2-1* plants: elongated pistil (I) and mature silique (J). K and L, Root epidermis and root tip (M), visualized by light microscopy. N, Root vascular tissues, visualized by confocal microscopy. Pictures were taken 23 (A–D and K–N), 30 (E and F), and 45 (G–J) d after sowing. Scale bars = 4 mm (A–D and G–I), 2 mm (E, F, and J), 200 μm (K, M, and N), and 100 μm (L).
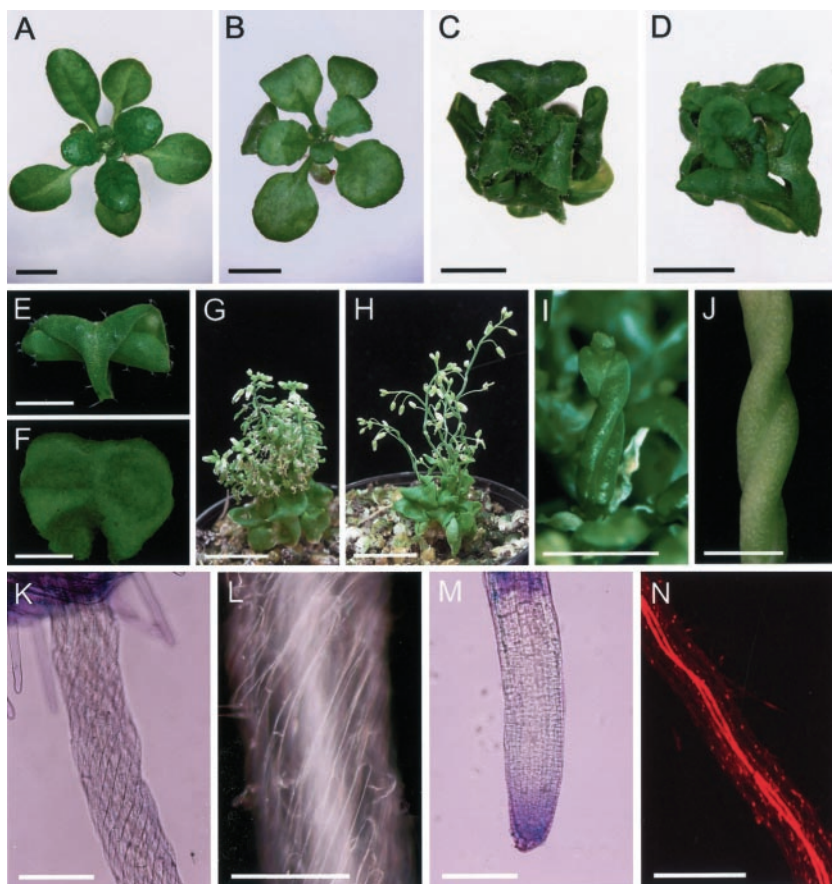
Pleiotropy of the Phenotype of *ucu2* Mutants

All the *ucu2* mutant alleles studied in this work displayed complete penetrance and only minor variations in expressivity. The rosette phenotypes of *ucu2-1*, *ucu2-2*, or *ucu2-3* homozygotes are indistinguishable (Fig. 1D) and very similar to the homozygotes for the *ucu1-1* and *ucu1-2* semidominant alleles of the *UCU1* gene (Fig. 1C).

Although the *ucu* mutants were isolated on the basis of the abnormal shape and size of their vegetative leaves, they display a pleiotropic phenotype. The *ucu2/ucu2* plants are dwarf, with shorter roots, hypocotyls, stems, and fruits than the wild type (Table I), compact dark-green rosettes (Fig. 1D), and reduced inflorescence length with partial loss of apical dominance (Fig. 1, G and H), traits also displayed by the homozygotes for the semidominant *ucu1* alleles (Fig. 1C; Table I; Pérez-Pérez et al., 2002). In addition, the three *ucu2* mutant alleles cause helical rotation of several radial organs, such as roots, hypocotyls, stems, and pistils, a trait that is clearly visible at whole-organ (Fig. 1, I and J) and epidermal cell level (Figs. 1, K and L). Confocal microscopy of hypocotyls and roots allowed us to visualize in addition the rotation of their internal tissues, such as the vasculature (Fig. 1N). Such spiral habits of growth in *ucu2/ucu2* plants caused the distortion of roots and stems, which are wavy and disorganized (Fig. 1H). Their flowers are small, and their pedicels, stamens, pistils, and siliques are twisted (Fig. 1, I and J). Some homeotic transformations of sepals and stamens into pistil tissues were also found. Fertility is reduced in these mutants, which is likely to be due to all the above-mentioned flower abnormalities.

The gravitropic response of the *ucu2* roots is similar to that displayed by the wild-type ones, as already shown in the *ucu1* mutants (Pérez-Pérez et al., 2002).

Root length is severely reduced, whereas root width is only slightly increased in the *ucu2* mutants (Table I), probably due to the helical rotation of this organ. The number of lateral roots of *ucu2/ucu2* plants was not found to be different from that of the wild type (data not shown). The helical rotation of primary and secondary *ucu2* roots is similar to that described above for the hypocotyls, as clearly shown in epidermal cells (Fig. 1, K and L) and vascular tissues (Fig. 1N). The apical region of *ucu2* roots does not display helical rotation of epidermal cells (Fig. 1M).

Leaf Architecture in the *ucu2* Mutants

The vegetative leaves of *ucu2/ucu2* plants show reduced expansion along the proximodistal axis (Fig. 1, D and E; Table I), which affects both the petiole and the lamina, and are indistinguishable from those of *ucu1-1* or *ucu1-2* homozygous plants (Fig. 1C; Table I). Their cauline leaves are reduced in length, wide, and very wrinkled (Fig. 1F) but do not display the circinate morphology of those of *ucu1/ucu1* plants.

When *ucu2/ucu2* leaves are stretched on a slide for observation under a microscope, their adaxial surface wrinkles, as occurred in the semidominant *ucu1/ucu1* mutants (Pérez-Pérez et al., 2002). The abaxial pavement cells of the *ucu2/ucu2* mutants (Fig. 2, B, F, and G), however, are only slightly smaller than those of the wild type (Fig. 2, A and E), unlike that observed in the *ucu1/ucu1* plants (Pérez-Pérez et al., 2002). No obvious differences with the wild type were found in the inner tissues of *ucu2/ucu2* leaves (Fig. 2, C–G), in contrast to *ucu1/ucu1* mutants, which showed a reduced number of air spaces (Pérez-Pérez et al., 2002). In addition, *ucu2/ucu2* leaves displayed many more

Table I. *Some body parameters of representative ucu mutants*

Values are means of at least 20 measurements ± SD. Lengths and widths are indicated in millimeters, and weights are indicated in milligrams.

Body parameters	Ler	ucu1-2/ucu1-2	ucu2-1/ucu2-1
Root length[a]	64.3 ± 9.0	27.5 ± 9.3	30.5 ± 9.4
Hypocotyl length (grown in the dark)[a]	25.5 ± 5.0	5.1 ± 1.4	15.3 ± 3.0
Number of vegetative leaves[b]	9.4 ± 0.6	9.5 ± 0.8	9.9 ± 0.9
Rosette diameter[b]	21.9 ± 4.3	7.6 ± 1.6	7.4 ± 1.6
Fresh weight[b]	24.4 ± 4.0	12.0 ± 3.7	9.4 ± 3.4
Dry weight[b]	1.9 ± 0.4	1.1 ± 0.5	0.8 ± 0.3
Petiole length[b]	4.4 ± 0.9	1.9 ± 0.5	1.3 ± 0.4
Lamina length[b]	7.3 ± 1.0	3.5 ± 0.5	2.8 ± 0.4
Lamina width[b]	5.7 ± 0.9	5.3 ± 0.5	4.0 ± 0.8
Pedicel length[c]	3.5 ± 1.1	1.6 ± 0.9	1.4 ± 1.2
Silique length[c]	8.5 ± 1.0	4.7 ± 0.9	ND[d]
Seeds per silique[c]	34.1 ± 5.2	13.4 ± 5.0	ND[d]
Primary stem length[c]	197.8 ± 30.9	59.9 ± 8.9	36.4 ± 12.6
No. of secondary stems[c]	2.1 ± 0.7	3.9 ± 0.9	6.2 ± 1.8

[a] Measurements were taken from plant material collected 11 d after sowing. [b] Measurements were taken from plant material collected 21 d after sowing. [c] Measurements were taken from plant material collected 49 d after sowing (see "Materials and Methods"). [d] ND, Not determined.
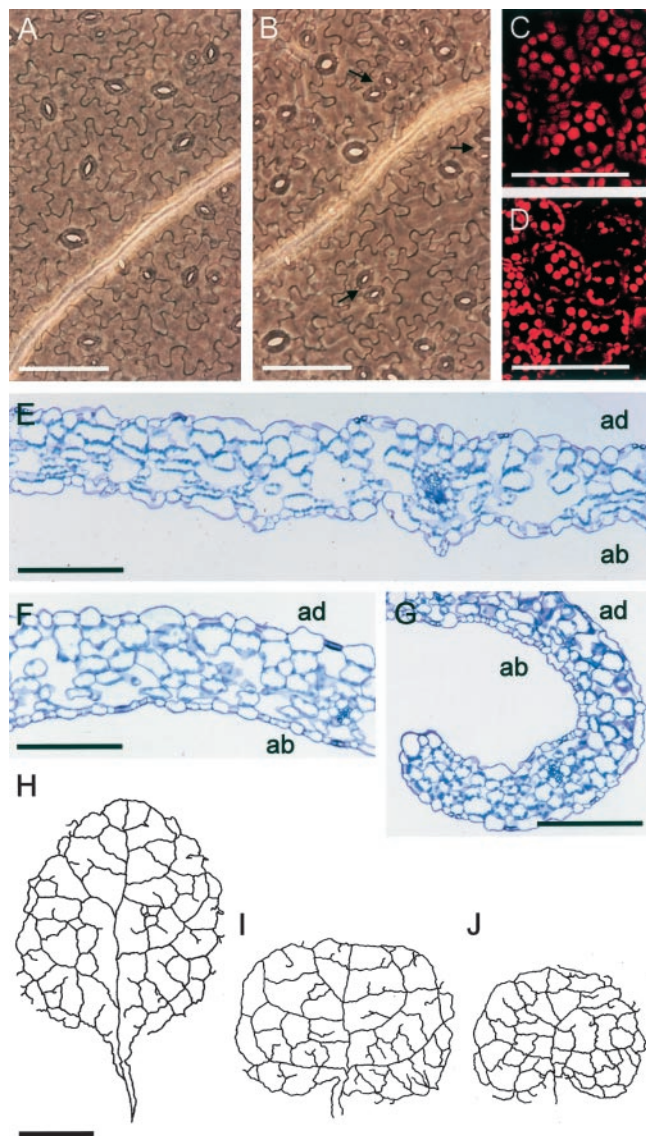
Figure 2. Ultrastructure of *ucu* mutant leaves. A and B, Micrographs of the abaxial epidermis. C and D, Confocal microscopy sections of third node vegetative leaves from the wild-type L*er* (A and C) and *ucu2-1/ucu2-1* (B and D) plants. Arrows indicate clustering of stomata in the abaxial epidermis of *ucu2-1/ucu2-1* leaves. E to G, Longitudinal sections of third node vegetative leaves of L*er* (E) and *ucu2-1/ucu2-1* (F and G) plants (F, basal region of the leaves; and G, apical regions of the leaves). Camera lucida drawings of the venation pattern of third node vegetative leaves of L*er* (H), *ucu1-2/ucu1-2* (I), and *ucu2-1/ucu2-1* (J) plants. Samples were collected 23 d after sowing. Scale bars = 100 μm (A–G) and 1 mm (H–J). ad, Adaxial, ab, abaxial.

clustered stomata than the wild-type leaves on both the adaxial and abaxial epidermis (Fig. 2, A and B).

Bending of the *ucu2/ucu2* vegetative leaves is more pronounced along the primary vein, whose length is clearly reduced compared with the wild type (Fig. 2, H and J), whereas the higher order veins and the complexity of the venation pattern seem to be much less affected, similar to that already observed in

plants homozygous for the *ucu1* semidominant alleles (Fig. 2I).

Physiological Analyses

The *ucu1* mutants display a de-etiolated phenotype similar to that of BR synthesis or response mutants (Pérez-Pérez et al., 2002). On the contrary, *ucu2/ucu2* plants grown in the dark displayed a wild-type photomorphogenic response because no leaves were developed (Table I; Fig. 3B). Although *ucu2/ucu2* hypocotyls were shorter than those of the wild type, their epidermal cells are not noticeably reduced in length along the proximodistal axis of the hypocotyls or in their width (Fig. 3A; data not shown).

We have shown previously that *ucu1* mutants are hypersensitive to auxin (Pérez-Pérez et al., 2002). The reduction in root length displayed by *ucu2/ucu2* plants grown in auxin-supplemented medium (20 or 50 nM 2,4-dichlorophenoxyacetic acid [2,4-D]) was similar to that found for the wild type (data not shown). Some phenotypic traits of the *ucu2/ucu2* plants, as the helical rotation displayed by some organs, are shared by mutants with disrupted auxin transport, such as *lop1* (*lopped1*; Carland and McHale, 1996). Hence, we analyzed the responses of *ucu2/ucu2* mutants to auxin transport inhibition by specifically blocking auxin influx with 1-naphthoxyacetic acid (1-NOA; Parry et al., 2001) or auxin efflux with NPA and TIBA (Fujita and Syono, 1996), in this way disrupting net polar auxin transport. Root growth was more inhibited by 1 μM NPA in the *ucu2/ucu2* mutants than in their wild-type backgrounds (Fig. 4A). Similar results were obtained when using 1 μM TIBA (data not shown). When grown in the presence of these auxin efflux inhibitors, *ucu2/ucu2* mutants also displayed an increase in root width and in the number and length of root hairs compared with the wild type. In addition, root hairs developed closer to the root apex in the *ucu2/ucu2* mutants than in the wild type (Fig. 3D). We found that these traits can be phenocopied in wild-type seedlings exposed to 50 nM 2,4-D. The aerial parts of *ucu2/ucu2* seedlings also displayed hypersensitivity to auxin efflux inhibitors (Fig. 3, E and F).

The *aux1/aux1* mutant plants, which are affected in the AUX1 permease-like protein, display agravitropic roots and disrupted auxin uptake (Bennett et al., 1996; Marchant et al., 1999). Phenocopies of *aux1/aux1* mutants can be obtained by treating wild-type plants with the auxin influx inhibitor 1-NOA, which does not affect root elongation (Parry et al., 2001). Although small concentrations of 1-NOA up to 10 μM abolish gravitropism in wild-type seedlings, thus phenocopying *aux1/aux1* mutants, this trait is unaffected in *ucu2/ucu2* seedlings. In addition, we found that the *ucu2/ucu2* mutants display a moderately reduced sensitivity to 24-epibrassinolide in root elongation assays (Fig. 4B), as already shown for the
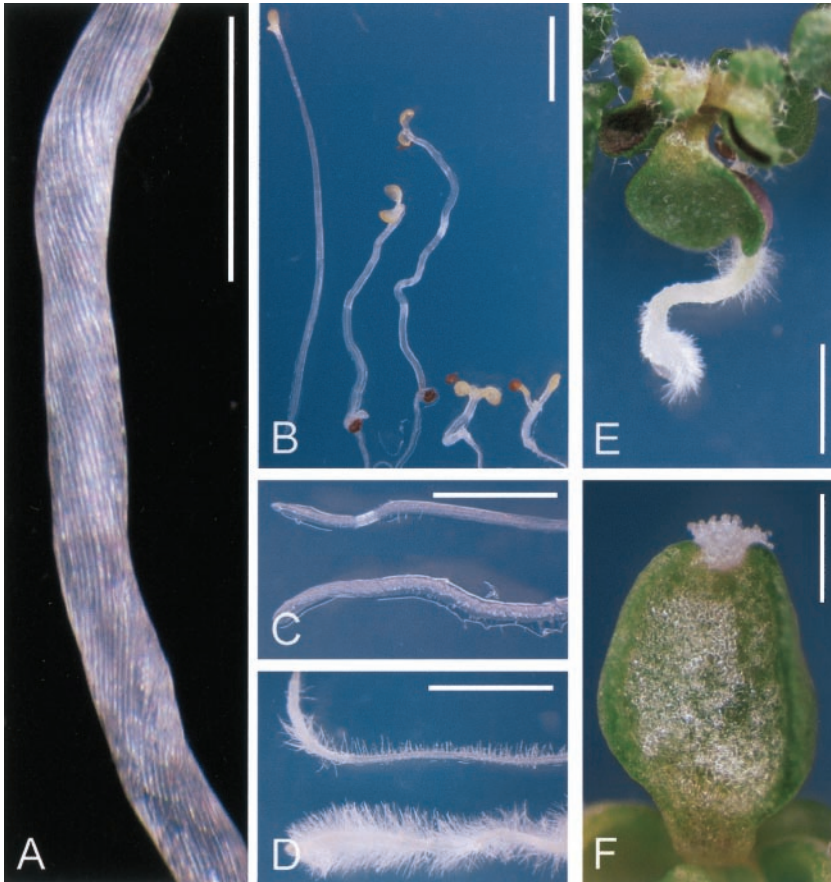
Figure 3. Physiological analyses of the *ucu2* mutants. A, *ucu2-3/ucu2-3* de-etiolated hypocotyl showing helical rotation of the epidermis. B, Photomorphogenic response of *ucu2* mutants when grown for 21 d in the dark. Left to right, Wild-type Col-0, *ucu2-1/ucu2-1*, *ucu2-3/ucu2-3*, *ucu1-2/ucu1-2*, and *det2-1/det2-1*. Although *ucu2-1/ucu2-1* and *ucu2-3/ucu2-3* display distorted hypocotyl growth, *ucu1-2/ucu1-2* and *det2-1/det2-1* show a characteristic de-etiolated phenotype. C, Roots of Col-0 (top) and *ucu2-3/ucu2-3* (bottom) plants. D, Col-0 (top) and *ucu2-3/ucu2-3* (bottom) roots grown on medium supplemented with 10 μM 1-N-naphthyl-phthalamic acid (NPA). E, *ucu2-3/ucu2-3* seedling grown on medium supplemented with 10 μM NPA. F, *ucu2-3/ucu2-3* heart-shaped cotyledon grown on medium supplemented with 10 μM 2,3,5-triiodobenzoic acid (TIBA), displaying apical tissue overgrowths. Pictures were taken 13 d after sowing. Scale bars = 1 mm (A and B) and 2 mm (C–F).

weak *ucu1-3* recessive allele of the *UCU1* gene (Pérez-Pérez et al., 2002).

Double Mutant Analysis

We obtained *ucu1/ucu1;ucu2/ucu2* double mutants (Fig. 5, A and B; Tables II and III) whose overall phenotype was in all cases the same irrespectively of the strength of the *ucu1* allele involved. Their rosette phenotype was strongly different from that of each *ucu/ucu* single mutant and quite similar to that of *bri1/bri1* plants (Fig. 5G). The BRI1 BR-receptor (Li and Chory, 1997) is upstream of the UCU1 (BIN2)

protein (Li and Nam, 2002; Pérez-Pérez et al., 2002) in the BR signal transduction pathway. The extreme rosette phenotype of the *ucu1-1/ucu1-1;ucu2/ucu2* double mutant (Fig. 5A) makes it difficult to determine whether or not it indicates additivity or synergy. However, the extreme rosette phenotype of the *ucu1-3/ucu1-3;ucu2/ucu2* double mutants (Fig. 5B) is clearly synergistic, given that it cannot be expected from the weak leaf phenotype of *ucu1-3/ucu1-3* single mutant plants (Fig. 1B).

Several dwarf mutants have been described as affected in BR biosynthesis (Altmann, 1999). These include *dim1* (Takahashi et al., 1995) and *det2* (Li et al.,
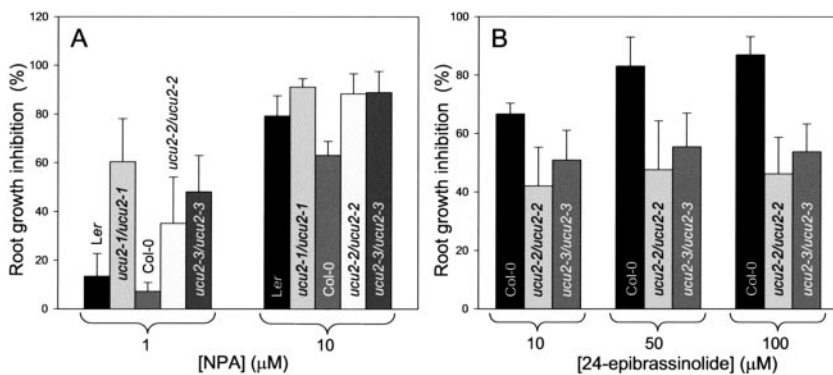
Figure 4. Response of the *ucu2* mutants to hormones. A, Root growth response to the auxin transport inhibitor NPA. B, Root growth response to 24-epibrassinolide. Each point in G and H represents mean data ($n > 15$) of the reduction in root length displayed by plants grown on hormone-supplemented media, compared with those grown on non-supplemented media.

Figure 5. Genetic interactions between *UCU2* and the *UCU1*, *DET2*, and *DIM1* genes. Rosettes from *ucu2-1/ucu2-1;ucu1-1/ucu1-1* (A) and *ucu2-1/ucu2-1;ucu1-3/ucu1-3* (B) double mutants. Inflorescence (C) and detail (D) of a helically rotated pistil of a *ucu2-1/ucu2-1;ucu1-1/ucu1-1* plant. *ucu2-1/ucu2-1;dim1-1/dim1-1* (E) and *ucu2-1/ucu2-1;det2-1/det2-1* (F) double mutant plants, which are extremely similar to the *bri1-1/bri1-1* mutant (G). Pictures were taken 23 (A, B, and E–G) and 45 (C and D) d after sowing. Scale bars = 4 mm (A, B, and E–G), 1 mm (D), and 1 cm (C).
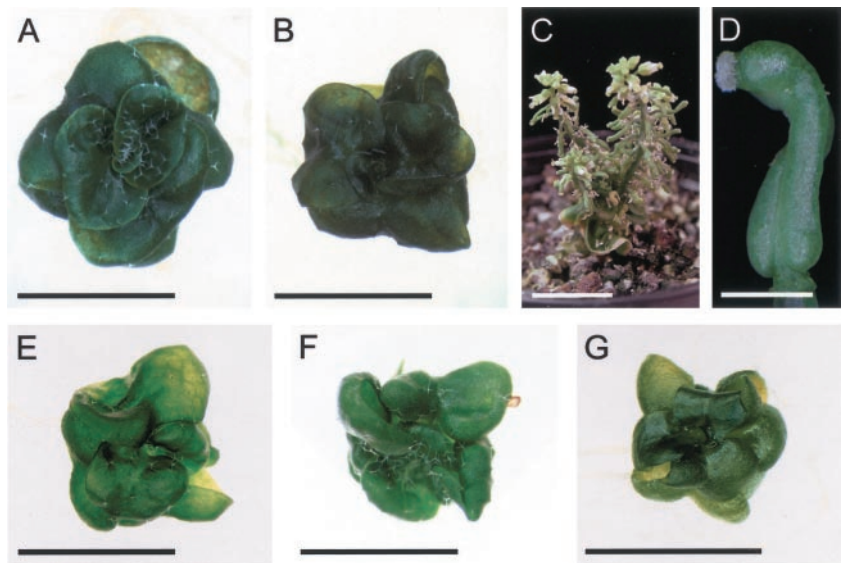
1996), which are specifically blocked in the early steps of the BR biosynthetic pathway. The *ucu2/ucu2; dim1/dim1* (Fig. 5E) and *ucu2/ucu2;det2/det2* (Fig. 5F) double mutants that we obtained displayed additive phenotypes similar to those of *bri1/bri1* mutants (Fig. 5G). The helical rotation characteristic of *ucu2/ucu2* organs was also displayed by all the double mutants obtained (Fig. 5D).

BR and Auxin-Induced Gene Expression

We tested whether exogenous 2,4-D or 24-epibrassinolide modulate the expression of several genes in the *ucu2* mutants (Fig. 6). To this end, several genes were chosen, all of them already described as regulated by plant hormones. This group of genes included the following (Table IV): *IAA7* (also named *AUXIN RESISTANT2*; *AXR2*) and *IAA2*, which are overexpressed in BR-deficient mutants and encode proteins of the Aux/indole-3-acetic acid (IAA) family (Nagpal et al., 2000; Liscum and Reed, 2002; Müssig et al., 2002) induced by IAA (Abel et al., 1995). *CPD* (*CONSTITUTIVE PHOTOMORPHOGENESIS AND DWARFISM*; Szekeres et al., 1996) and *ROT3* (*RO-*

TUNDIFOLIA3; Kim et al., 1998), which encode two cytochrome P450 enzymes involved in BR biosynthesis, both of them negatively regulated by BR (Mathur et al., 1998; Bancos et al., 2002); *CycD3* (*CyclinD3*), the product of which is involved in the progression of the cell cycle; and *BEE1* (*BRASSINOSTEROID ENHANCED EXPRESSION1*), which encodes a transcription factor. *CycD3* and *BEE1* are known to be induced by BR (Friedrichsen et al., 2002; Müssig et al., 2002). We studied also the expression of a gene that has no known relationship with BR or auxin signaling, *NCED3*, which codes for the 9-cis-epoxycarotenoid dioxygenase, one of the enzymes involved in abscisic acid (ABA) biosynthesis, whose expression is positively regulated by ABA (Xiong et al., 2002). Transcription of the *UCU1* gene was also studied.

Expression of the above-mentioned genes was analyzed by means of quantitative, real-time RT-PCR in *ucu2-1/ucu2-1* and *ucu2-3/ucu2-3* plants, together with their respective wild-type backgrounds L*er* and Col-0. In addition, we also studied *ucu1-2/ucu1-2* plants, the genetic background of which is L*er*. RNA was extracted from plants grown in liquid media

Table II. *Phenotypic segregations in the F$_2$ progeny of crosses involving ucu mutants*

Figures indicate the no. of plants belonging to a given phenotypic class. WT, Wild-type phenotype. UcuX, Ucul, and UcuW indicate extreme, intermediate, and weak Ultracurvata phenotype, respectively. UcuXH, Extreme Ultracurvata phenotype and helical rotation of some organs.

Cross (♀ × ♂)	F$_1$	F$_2$						
		WT	Ucul	UcuX	UcuXH	UcuW	Putative double mutants	χ^2
ucu2-1/ucu2-1 × ucu1-1/ucu1-1	38 Ucul	47	111	54	51	–	13	2.135[a]
ucu2-1/ucu2-1 × ucu1-2/ucu1-2	9 Ucul	54	104	60	56	–	14	1.778[a]
ucu2-1/ucu2-1 × ucu1-3/ucu1-3	30 WT	147	–	–	57	58	11	4.001[b]

[a] The χ^2 values represent the fit of the data (only families segregating for the putative double mutant are shown) to an expected 3:6:3:3:1 phenotypic segregation. [b] The χ^2 values represent the fit of the data (only families segregating for the putative double mutant are shown) to an expected 9:3:3:1 phenotypic segregation. Corresponds to a modified 3:6:3:1:2:1 segregation, given that the *ucu1-1/UCU1; ucu2-1/ucu2-1* and the *ucu1-1/ucu1-1; ucu2-1/ucu2-1* individuals were phenotypically indistinguishable

Table III. *Phenotypic segregations in the F_3 progeny of crosses involving ucu mutants*
  See Table 2 legend.

Cross (♀ × ♂)	F_2	F_3			
		UcuX	UcuW	Putative double mutants	χ^2 (3:1)
ucu2-1/ucu2-1 × *ucu1-1/ucu1-1*	UcuX	42	–	12	0.099
	UcuX	45	–	19	0.521
ucu2-1/ucu2-1 × *ucu1-2/ucu1-2*	UcuX	50	–	12	0.774
	UcuX	26	–	8	0.000
ucu2-1/ucu2-1 × *ucu1-3/ucu1-3*	UcuW	–	98	36	0.159
	UcuW	–	100	40	0.771

containing 50 nM 2,4-D or 100 nM 24-epibrassinolide and quantified by means of the comparative threshold cycle (C_T) method (Livak and Schmittgen, 2001), using the expression of the housekeeping *OTC* (*ORNITINE TRANSCARBAMILASE*) gene as an internal reference. We found no significant differences in the expression of the *NCED3*, *CycD3*, *BEE1*, and *UCU1* genes in the wild-type plants after auxin and BR treatment (data not shown). Hence, activity of these genes was not analyzed in the *ucu* mutants.

The *ucu1* and *ucu2* mutations do not affect induction by auxin of the *AXR2* and *IAA2* genes, as indicated by the similar strong effects of exogenous 2,4-D on the wild-type and mutant plants studied (Fig. 6, A and B). No remarkable effect of 24-epibrassinolide on *AXR2* and *IAA2* gene expression was observed. As expected, *ROT3* and *CPD* were found downregulated by brassinolide in the wild types studied, an effect that is abolished or extremely reduced by the *ucu2* mutations (Fig. 6, C and D). On the other hand, the expression of *ROT3* and *CPD* in the *ucu1* mutant studied was higher than in the wild type in noninductive conditions and did not change significantly by auxin or brassinolide treatment.

Isolation and Molecular Characterization of the *UCU2* Gene

Using an F_2 mapping population obtained from three *ucu2-1/ucu2-1* × Col-0 crosses, we determined the map position of the *UCU2* gene, which was found to be closely linked to the AtDMC1 (Klimyuk and Jones, 1997) cleaved-amplified polymorphic sequence marker (1.92 ± 0.57 cM, n = 574) in a region of 12.11 cM (1.9 Mb), flanked by the nga162 (8.35 ± 1.76 cM, n = 278) and AthGAPab (11.72 ± 2.12 cM, n = 252) markers (Fig. 7A). Allelism between *UCU2* and the *DIM* (Takahashi et al., 1995) and *AXR2* (Wilson et al., 1990) genes, the latter two mapping within the candidate interval, was ruled out after the corresponding complementation tests.

Based on the genome sequence available at Munich Information Center for Protein Sequences (MIPS; http://mips.gsf.de/proj/thal/db/index.html), we developed new simple sequence length polymorphism (SSLP) markers within the candidate region (Fig. 7B; Table V), which were used to screen for informative recombinants. The linkage analysis of 1,292 chromosomes performed using these new markers delimited the *UCU2* gene to an interval of 160 kb, encompassing three BAC clones (Fig. 7B). One of the candidate genes within this region, *At3g21650*, included in the MIL23 BAC clone, encodes a putative B′-regulatory subunit of a protein phosphatase 2A (PP2A B′-ζ; Terol et al., 2002), which displays 54% identity and 71% similarity to the human B56 PP2A protein delta isoform (NP_006236). The latter is known to inhibit Wnt signaling in a similar way to that in which it reduces the signaling of SHAGGY/GSK3 metazoan kinases, by reducing the transcription of Wnt-responsive genes by means of β-catenin degradation through ubiquitinylation (Seeling et al., 1999; Li et al., 2001b). Given the similarities between the phenotypes of *ucu1* and *ucu2* mutants and that *UCU1* encodes a SHAGGY/GSK3-like kinase (Pérez-Pérez et al., 2002), we considered *At3g21650* a strong candidate. Hence, several primer pairs were designed to PCR amplify the genomic region containing the *At3g21650* gene, but no amplification products were obtained from *ucu2-1/ucu2-1* or *ucu2-2/ucu2-2* genomic DNA. Because these results suggested a deletion, several primer pairs were designed for the adjacent gene, *At3g21640*, which codes for a putative FK506-binding protein (FKBP); once again, no PCR products were obtained. On the contrary, PCR products from both the *At3g21640* and *At3g21650* genes were obtained from the DNA of *ucu2-3/ucu2-3* plants, and no differences were found with the wild type in the coding region of the *At3g21650* transcription unit or in its 5′- and 3′-flanking regions. However, a rearrangement of 40 bp, including two small deletions in the 3′ region of the *At3g21640* gene, was shown to cause a frameshift and to induce a premature stop codon in the *ucu2-3/ucu2-3* mutant. In addition, we found by RT-PCR that the *At3g21640* gene is expressed in *ucu2-3/ucu2-3* plants, although its transcript is smaller than that of the wild type (Fig. 7D).

To determine the nature of the alterations carried by the *ucu2-1/ucu2-1* and *ucu2-2/ucu2-2* mutants, we performed a Southern blot using three probes spaced along the region of the MIL23 BAC clone including *At3g21640* and *At3g21650* (probe 3) and their two flanking genes, *At3g21630* (probe 1) and *At3g21660*
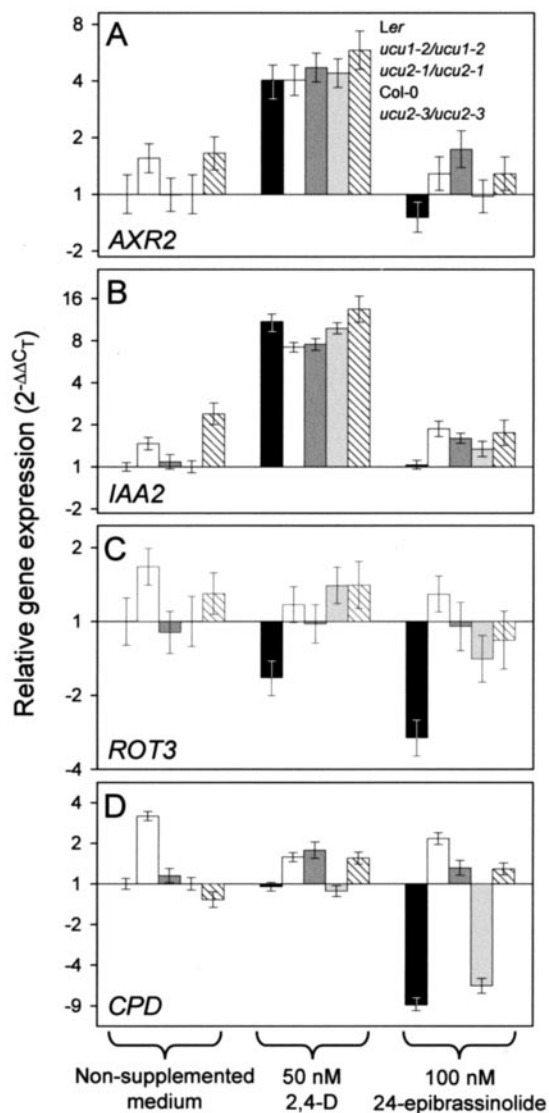
Figure 6. Real-time reverse transcriptase (RT)-PCR quantification of the expression of several genes in the *ucu1* and *ucu2* mutants. The expression of *AXR2* (A), *IAA2* (B), *ROT3* (C), and *CPD* (D) genes was studied in the presence of exogenous auxin (50 nM 2,4-D) or BR (100 nM 24-epibrassinolide) and compared with their expression under noninductive conditions in the wild type. Relative expression was normalized as regards to that of the *OTC* gene (see "Materials and Methods").

(probe 2; Fig. 7E). No differences with the wild type were found for the genomic DNA of *ucu2-3/ucu2-3* plants (Fig. 7E). In regards to *ucu2-1*, no hybridization bands were detected with probes 2 and 3, whereas the bands obtained with probe 1 were different from those of the wild type, suggesting the deletion of about 6 kb, which removes the *At3g21640*, *At3g21650*, and *At3g21660* genes. In regards to *ucu2-2*, no hybridization bands were detected when using probes 1 and 3, but probe 2 revealed bands different from those of the wild type, suggesting that this mutant suffers a deletion encompassing the

At3g21630, *At3g21640*, and *At3g21650* genes. In addition, RT-PCR analyses confirmed the absence of the *At3g21640* transcription product (data not shown) in *ucu2-1/ucu2-1* and *ucu2-2/ucu2-2* plants (data not shown).

Complementation of the Mutant Phenotype of *ucu2-3/ucu2-3* Plants

With the aim of confirming that the lack of function of the *At3g21640* gene is responsible for the phenotype of *ucu2* mutants, a segment of 2,441 bp of the genomic region harboring this gene, including its whole coding region, which contains 1,235 bp of the 1,360-bp full-length cDNA, was cloned into the binary vector pART27 (see "Materials and Methods") under the control of a *35S* promoter. Homozygous *ucu2-3* plants were transformed with the *35S: At3g21640:ocs* construct, and the T_2 progeny obtained was sown on kanamycin-supplemented medium. Six transformants were isolated, which unambiguously displayed wild-type vegetative and cauline leaf phenotypes, normal length of the stem and siliques, and no helical rotation of organs (Fig. 8A). The phenotypic segregations observed in their T_3 progeny (Table VI) suggested that the T_2 plants were as expected, hemizygous for the transgene. Furthermore, the presence of the *35S:At3g21640:ocs* transgene in the T_2 plants was confirmed by amplification of the segment of the *At3g21640* gene that is deleted in the *ucu2-3* allele (Fig. 8B).

In addition, we screened T-DNA collections for additional alleles of the *UCU2* gene. The Salk_012836 insertion line from the Salk Institute Genomic Analysis Laboratory (SIGnAL) collection carries a T-DNA insertion in the fifth exon of *At3g21640*. Its mutant phenotype is indistinguishable of that of *ucu2* mutants and was inherited as a recessive trait (Fig. 8C). We named this allele *ucu2-4*.

The *UCU2* Gene Encodes the FKBP42 of Arabidopsis

The *At3g21640* gene codes for a protein with homology to the FKBP type of PPIases (or rotamases; E.C. 5.2.1.8). Its mRNA is 1,360 nucleotides long (AJ224640), with an open reading frame of 1,095 nucleotides that gives rise to a protein of 365 amino acids and 42 kD, nine amino acids different from the At3g21640 gene, as annotated in the MIPS genome project Web page (http://mips.gsf.de/proj/thal/db/index.html), probably as the result of the incorrect deduction of the splicing site. The *UCU2* gene consists of eight exons, and the UCU2 protein shows significant similarity with the FKBP-type immunophillins (Galat, 2000), which are characterized by a conserved FKBP-like domain carrying the PPIase activity (Schiene-Fischer and Yu, 2001). When we compared the UCU2 amino acid sequence with those of already known FKBPs, we found a single PPIase

Table IV. *Quantitative RT-PCR primer pairs used in this work*

Gene	Bacterial Artificial Chromosome (BAC)	Oligonucleotide Sequences (5′ → 3′)		PCR Product Size (bp)
		Forward primer	Reverse primer	
CPD (At5g05690)	M3J3	CTCAACTCAAGGAAGAGCATGA	GTGTGAATGGCATTGACTTGTAAT	93
CycD3 (At1g43680)	F28A23	TCTGTAATCTCCGATTCAAGATT	GCTCTATAATTCGCATCATGGTA	79
ROT3 (At1g43680)	F24P17	AAAGTCTTTATACGGGAAAGTGTT	ACCACTTTATTCACCTCTGCAT	87
BEE1 (At1g18400)	F15H18	CACTGAAACAGGTTCTTTGAGAA	GGCCTCTTCTGGCTCTCACA	104
IAA2 (At3g23030)	MXC7	TACACCTCCTACCAAAACTCAA	CTTTCACGTAGCTCACACTGTT	86
UCU1 (At4g18710)	F28A21	GAGATCTAAAGCCTCAAAATCTT	TGGCTTCACCTTTAACGAGCT	99
AXR2 (At3g23050)	MXC7	GCTCCTTTACTATGGGAAACTAT	TACTCAGAGCTATTCAGCAGATT	91
NCED3 (At3g14440)	MOA2	CGGTGGGTTTACGACAAGAACAA	CAGAAGCAATCTGGAGCATCAA	103
OTC (At1g75330)	F1B16	TGAAGGGACAAAGGTTGTGTATGTT	CGCAGACAAAGTGGAATGGA	95

domain that includes amino acids 58 to 156. The C-terminal region of UCU2 contains three putative domains of the tetratricopeptide repeat (TPR) type, a 34-amino acid domain involved in protein-protein interactions, which mediates association into multi-protein complexes (Blatch and Lassle, 1999). When

the amino acid sequence of UCU2 was compared with those of proteins found in databases, the highest degree of similarity was observed with other FKBPs: 50% similarity and 34% identity with the FKBP1 Rotamase (ROF1; Vucich and Gasser, 1996; S72485) and 46% similarity and 28% identity with PASTIC-
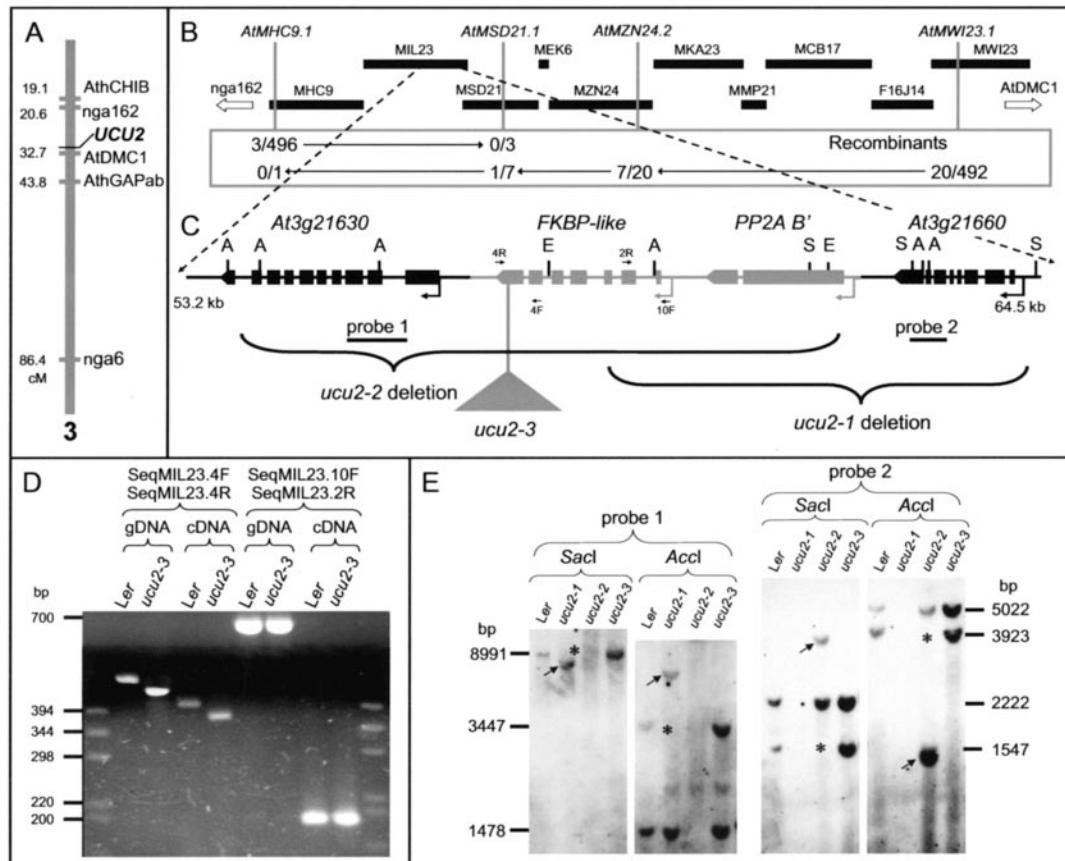
Figure 7. Positional cloning of the *UCU2* gene. A, Map position of the *UCU2* gene as determined by low-resolution mapping. B, Physical map of the BAC contig assumed to contain the *UCU2* gene. A total of 23 recombination events were identified relative to four molecular markers (those shown in italics) within this region. C, Candidate region with indication of the mutations found in the *ucu2* mutants. Boxes, Exons; lines between boxes, introns. A, S, and E, Positions of restriction sites for *Acc*I, *Sac*I, and *Eco*RI, respectively, for the enzymes used for the Southern blot shown in E. D, Amplification products corresponding to the *At3g21640* gene, obtained using the primers indicated at the top and genomic DNA (gDNA) or cDNA as a template, from wild-type (L*er*) and *ucu2-3* homozygous (*ucu2-3*) plants. The positions of the primers used within the region containing the *At3g21640* gene are indicated as 4R, 4F, 2R, and 10F in C. E, Gel blots of genomic DNA from the *ucu2* mutants hybridized with probes 1 and 2. The results shown were obtained by reprobing a single membrane. The absence of some bands is indicated by asterisks, and the differential bands present in the DNA of the mutants are indicated by arrows.

Table V. *Novel SSLP primer sets used in this work*

Marker	BAC	Position in BAC	Oligonucleotide sequences (5′ → 3′)		PCR Product Size (bp)	
			Forward labeled primer	Reverse primer	Ler	Col-0
AtMHC9.1	MHC9 (AP001305)	3,316–3,716	ACAGAGGAACAATTGATCTCATC[a]	TCACAGGAAACTCTGAGAAACG	448	400
AtMSD21.1	MSD21 (AB025634)	29,271–29,544	GTAGATATTATACATGTAACATTCG[b]	TTAAAAACGGTAAGGTAGTTATTAC	247	274
AtMZN24.2	MZN24 (AB028622)	69,687–69,707	ATCAACTGGAAGCACTTGCGC[c]	TGAGGTGTTTGCCGATCTACG	230	240
AtMWI23.1	MWI23 (AB022223)	52,271–52,588	GAAGCCTTAGTAATGCACCGG[b]	GATTGTGCATCCTTTGGCTGC	318[d]	354[d]

[a] Primer pair included an oligonucleotide labeled with 4,7,2′,4′,5′,7′-hexachlo-0-6-carboxyfluorescein phosphoramidites.   [b] Primer pair included an oligonucleotide labeled with 6-carboxyfluorescein phosphoramidites.   [c] Primer pair included an oligonucleotide labeled with 4,7,2′,7′-tetrachloro-6-carboxyfluorescein phosphoramiotes. Primers were designed based on the Col-0 genomic sequence data available at MIPS (http://mips.gsf.de/proj/db/index.html)   [d] Sizes were determined by sequencing the corresponding amplification products, which were found to contain 15 and nine TGGAGG repeats in the Col-0 and Ler accessions, respectively. In contrast to the Col-0 genomic sequence annotated at MIPS, which has been reported not to be different from that of Ler.

CINO1 (AL132960), both of them of Arabidopsis; 50% similarity and 32% identity with a 77-kD FKBP of wheat (*Triticum aestivum*; wFKPB77; T06489), and 52% similarity and 29% identity with a 59-kD FKBP of mouse (*Mus musculus*) (AAH03447). All of these FKBPs contain three PPIase domains, in contrast to the single PPIase domain of UCU2, which includes five putative phosphorylation sites and several *N*-myristoylation sites that may correspond to posttranslational modifications. An unusual characteristic of the UCU2 protein when compared with already known immunophilins of the FKBP type is a putative transmembrane region in its C terminus that is absent from other FKBP-like proteins.

The small DNA rearrangement of the *UCU2* gene found in the *ucu2-3* allele causes a frameshift that abolishes the third TPR domain and the putative transmembrane domain at the C terminus, as a consequence of the appearance of a premature stop codon. Because the *ucu2-3* mutation does not affect transcription of the *UCU2* gene, the similarity between the phenotypes of *ucu2-1* and *ucu2-2*, which are null alleles, and *ucu2-3* clearly indicates that the C-terminal region is required for the activity of UCU2.

DISCUSSION

Morphology of the *ucu* Mutants

Here, we present a genetic and molecular analysis of four recessive alleles of the *UCU2* gene, which cause the mutant plants to be dwarf and to display circinate vegetative leaves and helical rotation of some organs. The circinate leaf phenotype of the *ucu1* and *ucu2* mutants is presumably the consequence of a perturbation in the coordination of the growth of the adaxial and abaxial tissues along the proximodistal leaf axis. Histological analyses of *ucu2/ucu2* leaves indicated that they might be defective in the differentiation of the primary vein. In fact, leaf morphology is severely altered in venation pattern mutants (Koizumi et al., 2000; Semiarti et al., 2001) and in wild-type plants treated with auxin transport inhibitors (Mattsson et al., 1999; Sieburth, 1999). A reduction in primary vein length was also observed in the *ucu1* mutants (this work), which is consistent with the abaxial origin of these tissues. Although we have shown previously that the *ucu1* mutants display differences in cell size between the abaxial and adaxial epidermis (Pérez-Pérez et al., 2002), no such differences were found in the mutant leaves of *ucu2/ucu2* plants.

The small size of most organs is a phenotypic trait shared by the *ucu* mutants and BR-deficient or -insensitive mutants. The leaf morphology of *ucu* mutants, however, is rather different from that of all other dwarf mutants affected in BR synthesis or perception, whose small rounded leaves suffer a significant reduction in both cell size and cell number in all the tissues studied (Nakaya et al., 2002). Both the vegetative and cauline leaves of *ucu* mutants are reduced in length but retain a normal width, which indicates that the expansion of the organ in these mutants is reduced along the proximodistal axis but

Figure 8. Functional complementation of an *ucu2* mutation. Wild-type phenotype of *ucu2-3/ucu2-3;35S:At3g21640:ocs* transgenic plants (A). B, PCR amplification products obtained using primers flanking the *At3g21640* transcription unit and DNA extracted from: lane 2, Ler; lane 7, *ucu2-3/ucu2-3*; and lanes 3 to 6, *ucu2-3/ucu2-3;35S:At3g21640:ocs* transgenic plants. C, *ucu2-4/ucu2-4* mutant plant. Pictures were taken 23 d after sowing. Scale bars = 4 (A) and 2 (C) mm.

Table VI. *Segregation of kanamycin resistance in the progeny of ucu2-3/ucu2-3 plants subjected to transformation*

See Table 2 legend. Kan^R and Kan^S, Kanamycin-resistant and -sensitive individuals, respectively.

Transgene Used	T_2	T_3					
		Non-supplemented medium			Supplemented medium		
		WT	UcuX	χ^2 (3:1)	Kan^R	Kan^S	χ^2 (3:1)
35S:At3g21640:ocs	WT	77	34	1.589	142	63	0.063
	WT	76	38	3.789	100	58	2.364
	WT	70	32	1.882	98	48	4.898
	WT	140	50	0.112	84	47	1.528
	WT	59	24	0.486	63	23	3.172
	WT	21	8	0.011	48	19	0.065

not along the mediolateral axis. In addition, the *ucu2* mutants displayed an etiolated phenotype when grown in the dark, contrary to that shown by BR-deficient and -insensitive dwarf mutants, which indicates that *ucu2* mutants are not affected in the repression by darkness through the BR signaling pathway of the light-induced developmental program.

Only recently has the genetic analysis of Arabidopsis mutants shed light on the molecular components of handedness in plants, by the identification of genes involved in establishing left-right asymmetry patterns (Hashimoto, 2002). A number of mutants with a helical habit of growth have been identified, including *lefty1* and *lefty2*, which are affected in the genes that encode the TUA6 and TUA4 α-tubulins, both of them involved in cortical microtubule orientation (Thitamadee et al., 2002). These results, together with the observation that proper orientation of microtubule arrays is disrupted in the *spiral* mutants (Furutani et al., 2000), indicate the importance of microtubule organization in establishing helical handedness in Arabidopsis. Plant hormones such as auxins and BR, among others, can perturb plant morphology through microtubule reorientation (Catterou et al., 2001). It must be noted, however, that the helical rotation found in the *ucu2* mutants only affects organs that present radial symmetry in the wild type, whereas all organs are rotated in other helical mutants. No helical rotation has been shown in any BR-deficient mutants described to date (Catterou et al., 2001).

The helical rotation displayed by *ucu2* mutants might be related to that caused by mutant alleles of the *LOP1* (*LOPPED1*) gene (Carland and Hale, 1996), also named *TRN1* (*TORNADO1*; Cnops et al., 2000). Such *lop1* and *trn1* mutants display a pleiotropic phenotype, which is characterized by a perturbation in leaf vasculature and abnormal patterns of cell expansion that cause helical rotation of the root and deformed leaves, including twisting of the petiole (Carland and McHale, 1996). The phenotype of the *lop1* mutants seems to be caused by deficiencies in the basipetal transport of IAA (Carland and McHale, 1996). The maize *rs2* (*rough sheath2*) mutant, which

displays aberrant leaf vasculature development and dwarfism, was also found to be defective in the basipetal transport of auxin in the shoot (Tsiantis et al., 1999).

The *UCU2* Gene Encodes an FKBP

To gain insight into the molecular nature of the UCU2 function, we positionally cloned the *UCU2* gene, which was found to encode an Arabidopsis FKBP. FKBPs belong to the PPIase family of folding proteins, also named rotamases, whose homologs are found in prokaryotes, such as *Escherichia coli*, and eukaryotes such as yeast, invertebrates, mammals, and plants (Galat, 2000). Low-M_r FKBPs participate in signal transduction pathways through association with transmembrane receptors and usually include a single PPIase domain, similar to that found in the UCU2 protein. An example of this is mammalian FKBP12, which has been found to be associated with the TGF-β type II receptor and calcium channels (Schiene-Fischer and Yu, 2001). Multidomain PPIases are characterized by their C-terminal domain, which binds calmodulin and interacts with multiple partners (Schiene-Fischer and Yu, 2001). The multidomain PPIase FKBP52 (52-kD mammalian FKBP) is associated with Hsp90 through its TPR domain and participates in the activation of the cytoplasmic glucocorticoid receptor complex and its migration into the nucleus (Galigniana et al., 2001; for review, see Pratt et al., 2001). It has been demonstrated recently that plants hold the entire heterocomplex assembly machinery that links the glucocorticoid receptor complex to dynein, the motor protein that guides the complex to the nucleus (Harrell et al., 2002). Furthermore, wheat plants overexpressing wFKBP77 showed dwarfism, sterility, and altered leaf shape (Harrar et al., 2001). The UCU2 protein is a high-M_r FKBP that includes three TPR domains but only one PPIase domain, hence sharing structural properties with both previously known classes of FKBPs.

We found the UCU2 protein to be the same as AtFKBP42, some of whose functional characteristics have been reported recently (Kamphausen et al., 2002), including its localization in the plasma mem-

brane and in the tonoplast and the interaction of its TPR domain with the COOH-terminal region of the heat shock protein, Hsp90. Such an interaction with Hsp90 is similar to that already shown for other FKBPs (Owens-Grillo et al., 1996; Young et al., 1998) as the mammalian PPIases, FKBP51 and FKBP52, which is necessary for the maturation of nonactivated steroid hormone receptor complexes (Richter and Buchner, 2001). AtFKBP42 also may be part of an analogous steroid hormone receptor complex in Arabidopsis, probably through their interaction with the BRI1 BR receptor. No PPIase activity has been detected for AtFKBP42 (Kamphausen et al., 2002), in contrast to that found for mammalian FKBP51 and FKBP52 (Schiene-Fischer and Yu, 2001). At least another FKBP, FKBP71, is known to be involved in the development of Arabidopsis. Mutations in the *PAS1* (*PASTICCINO1*) gene, which encodes the FKBP71 (Vittorioso et al., 1998), display altered cell division and elongation, probably as a consequence of the perturbation of cytoquinin signaling (Faure et al., 1998).

All the *ucu2* alleles studied here are likely to be null, given that the *ucu2-1* and *ucu2-2* mutants carry a deletion of the whole *At3g21640* gene and that their mutant phenotypes are indistinguishable from that of *ucu2-3* and *ucu2-4*. The deletion of the *At3g21630* and *At3g21650* genes in the *ucu2-1* mutant and that of *At3g21650* and *At3g21660* in the *ucu2-2* mutant do not cause a visible phenotype, possibly due to gene redundancy. The *At3g21650* gene, for instance, codes for the PP2A B'-ζ, which has at least seven paralogs in the genome of Arabidopsis (Terol et al., 2002).

Auxin and BR Responses Are Perturbed in the *ucu* Mutants

A large body of evidence supports the hypothesis of a connection between the auxin and BR signaling pathways. Some auxin-regulated genes, such as *Aux/IAA* and *ARF* (*AUXIN RESPONSE FACTOR*) genes, have been found overexpressed in BR-deficient mutants (those of *ARF7*, *AXR3* [*IAA17*], *SHY2* [*IAA3*], *IAA2*, *AXR2* [*IAA7*], and *IAA22* genes), or expressed in response to BR (such as *IAA3* and *IAA19*; Müssig et al., 2002). In addition, altered responses to auxins have been described in some BR-deficient or -insensitive dwarf mutants, such as in the *curl-3* tomato (*Lycopersicon pimpinellifolium*) mutant, which is hypersensitive to 2,4-D and is affected in a homolog of the BRI1 receptor (Koka et al., 2000; Bishop and Koncz, 2002), in the *sax1* (*hypersensitive to ABA and auxin1*) mutant, whose hypersensitivity to auxin is restored after BR treatment (Ephritikhine et al., 1999a; 1999b) or in the *ucu* mutants (Pérez-Pérez et al., 2002; this work). A reduction of IAA levels was also observed in the BR-deficient *lkb* mutants of pea (*Pisum sativum*; Nomura et al., 1997).

Our results on the morphological, physiological, and genetic analysis of the *ucu* mutants of Arabidop-

sis indicate the implication of the *UCU* genes in the signaling pathways of auxin and BRs. Further support to this hypothesis is given by the quantitative differences found between the *ucu1* and *ucu2* mutants and the wild types studied here with regard to the effects of 24-epibrassinolide on the expression of the *CPD* and *ROT3* genes, which are involved in BR biosynthesis. Down-regulation by exogenous BR of *CPD* and *ROT3* is abolished by the *ucu1* and *ucu2* mutations, which indicates that *UCU1* and *UCU2* are required for BR-regulated gene expression.

Our auxin transport inhibition analyses suggest that *UCU2* might be involved in the regulation of the transport of auxin. Contrary to that expected from the hypersensitivity displayed by the *ucu1* mutants to auxin (Pérez-Pérez et al., 2002) and by the *ucu2* mutants to auxin transport inhibitors (this work), auxin-induced expression of *AXR2* and *IAA2* genes was found to be similar in the wild-type and in the *ucu* mutants. Further analyses will be required to ascertain whether or not the growth responses of the *ucu* mutants to exogenous auxin or auxin transport inhibitors are mediated by the *AXR2* and *IAA2* genes.

It has been proposed that ATP-binding cassette (ABC) plant proteins, which are related to those of the multidrug resistance (MDR) family of animal proteins (often referred to as P-glycoproteins), could be involved in auxin transport in plants (Gaedeke et al., 2001; Noh et al., 2001; Luschnig, 2002). Support for this hypothesis is provided by mutant alleles of the *AtMDR1* gene, which are defective in basipetal auxin transport and cause epinastic cotyledons and wrinkled leaves (Noh et al., 2001). Furthermore, the phenotype of a double mutant lacking both *AtMDR1* and its closest homolog *AtPGP1* (Noh et al., 2001) is similar to that of the *ucu2* mutants described in this work, with a dwarf phenotype, leaves curled down, and a distorted habit of growth.

AtMDR1 and AtPGP1 are likely to be required for auxin efflux, preventing excessive auxin accumulation (Luschnig, 2002). In a similar way, the *ucu2* epinastic leaf phenotype can be explained by the accumulation of intracellular auxin as a result of a defect in its polar transport, either directly if UCU2 participates in the auxin transport complex or indirectly through the posttranslational modification of the AtMDRP1 and AtPGP1 transporters. The analysis of *ucu2/ucu2;atpgp1/atpgp1;atmdr1/atmdr1* triple mutants would help to test such a hypothesis. It is known that FK506 immunosuppressant drugs are able to inhibit P-glycoprotein-mediated MDR in mammals, which suggests that FKBPs might positively regulate ABC transporter function (Hemenway and Heitman, 1996). Increased auxin levels have been found in the *atmdr5* mutants of Arabidopsis. The wild-type ABC transporter AtMRP5 is also able to transport organic anions when expressed in yeast, such as estradiol-17-(β-D-glucuronide), a product of the catabolism of steroids in animals (Gaedeke et al.,

2001). Furthermore, a role as a steroid transporter has been reported for the human P-glycoprotein (Ueda et al., 1992).

UCU1 and UCU2 Function and Interaction

The similarity between the leaf phenotypes of *ucu1* and *ucu2* mutants, together with their insensitivity to BR, prompted us to consider the possibility that the *UCU1* and *UCU2* genes participate in some developmental process related with BR signal transduction. We found that the phenotype of *ucu1 ucu2* double mutants is indistinguishable from that of *bri1* single mutants, which suggests that UCU1 and UCU2 act in convergent pathways, both probably downstream of the BRI1 receptor, to cooperatively trigger BR responses. The UCU2 protein can be a positive regulator of BR signaling, acting by controlling hormone transport through ABC transporters. Another possibility is that UCU1 and UCU2 participate in the same pathway and that the semidominant, gain-of-function *ucu1* alleles interfere with the function of UCU2.

Recessive mutations in the *AXR1* gene confer resistance to auxin and cause morphological alterations, such as wrinkled leaves. *AXR1* encodes a protein related to the ubiquitin-activating enzyme E1, which is a key component in a complex that controls ubiquitin-mediated protein stability (Leyser et al., 1993). In addition, it is known that alterations in the ubiquitin pathway, caused by overexpressing a modified ubiquitin that inhibits protein degradation, could originate curled down leaves in tobacco (*Nicotiana tabacum*; Bachmair et al., 1990). Furthermore, the auxin efflux carrier EIR1 (also named AGR or At-PIN2), which is involved in the gravitropic response of roots, is posttranscriptionally modified and requires the function of AXR1, suggesting that auxin transport is regulated through protein stability (Sieberer et al., 2000). UCU1 (BIN2) is likely to be a negative regulator of the BR transduction pathway, acting through the destabilization of the BES1 and BZR1 transcription factors (He et al., 2002; Yin et al., 2002). Such negative regulation may be dependent on protein degradation mediated by ubiquitin, which is analogous to protein degradation mediated by of SGG/GSK3 in the Wingless/Wnt pathway of metazoans (Barker et al., 2000; Clouse, 2002). On the other hand, metazoan SGG/GSK3 kinases regulate signaling pathways other than that of Wingless/Wnt, such as those of insulin or cell cycle control (for review, see Cohen and Frame, 2001). It has been described recently that BRI1 interacts with BAK1, another Leu-rich repeat receptor-like protein kinase, which suggests a conserved downstream activation pathway between BR signal transduction in plants and the TGF-β signaling cascade in metazoans (Li et al., 2002). In fact, the interplay between the TGF-β and Wingless/Wnt signaling pathways is important for the specification of cell fates during animal development (Capdevila and Izpisúa-Belmonte, 2001). If a similar cross talk between pathways occurs in plants, the phenotype of *ucu1 ucu2* double mutants might suggest the implication of both UCU1 and UCU2 in an interaction between the BRI1 pathway and the activation of the ABC transporters. This would explain the similarities of *ucu1* and *ucu2* leaf phenotypes and their phenotypic differences with BR-deficient or -insensitive mutants.

A role for the *UCU2* gene can be proposed in the cross talk between the auxin and BR signal transduction pathways, which would be achieved primarily by regulation of auxin homeostasis through activation of one or both of the AtMDR1 and AtPGP1 ABC transporters or by the regulation of the BRI1 and BAK1 heterocomplex. Further molecular analyses will be required to gain insight into such a mechanism of cross talk between plant hormones.

MATERIALS AND METHODS

Plant Materials and Growth Conditions

Seeds from Arabidopsis L*er* and Col-0 accessions were supplied by the Nottingham Arabidopsis Stock Center (Loughborough, UK). The CS3397 line and the *DIM1/dim1-1* (CS8100), *det2-1/det2-1* (CS6159), *BRI1/bri1-1* (CS3723), *aux1-7/aux1-7* (CS3074), and *axr2-1/axr2-1* (CS3077) mutants were supplied by the Arabidopsis Biological Resource Center (Ohio State University, Columbus). The *ucu2-1* and *ucu2-3* alleles, respectively, were isolated after fast neutron mutagenesis in a L*er* background (P. Robles and J.L. Micol, unpublished data) and T-DNA mutagenesis in a Col-0 background (this work). The N512836 insertion line (*ucu2-4/ucu2-4*) was supplied by the Nottingham Arabidopsis Stock Center and is described at the SIGnAL Web site (http://signal.salk.edu). The nomenclature rules of Meinke and Koornneef (1997) for phenotypes, genes, alleles, mutations, and proteins are followed in this paper.

Cultures were performed as described by Ponce et al. (1998), at 20°C $\pm$ 1°C and 60% to 70% relative humidity under continuous illumination of 7,000 luxes. Crosses were performed as described by Berná et al. (1999).

Photomicrography and Morphometric Analysis

Morphometric analyses of *ucu2* mutants were carried out as described previously (Candela et al., 1999; Pérez-Pérez et al., 2002). Photographs were taken with a Cybershot FV-505 digital camera (Sony, Tokyo) using a resolution of 1,024 × 768 pixels. Photomicrography and confocal microscopy of whole leaves and leaf sections were performed as described by Serrano-Cartagena et al. (2000) and Pérez-Pérez et al. (2002). Images were digitally processed with the Adobe Photoshop 6.0 program (Adobe Systems Incorporated, San Jose, CA).

Physiological Analyses and Hormone Treatment

Photomorphogenic and gravitropic responses were studied as described by Pérez-Pérez et al. (2002). Photomorphogenic development was monitored 13 and 21 d after sowing.

For the root elongation assays of hormone-treated plants, at least 30 seedlings of each genotype were grown in vertically oriented agar plates supplemented with 0, 10, 50, or 100 nM epibrassinolide (no. E1641, Sigma, St. Louis), a mixture of synthetic BR; 0, 10, 20, or 50 nM 2,4-D (no. 11215-019, Life Technologies/Gibco-BRL, Cleveland), a synthetic auxin; 0, 1, 5, or 10 μM TIBA (no. T5910, Sigma) or NPA (no. 34361, Riedel-de-Häen, Seelze, Germany), two auxin efflux transport inhibitors; and 0, 1, 5, or 10 μM 1-NOA (no. 25,541-6, Aldrich, Milwaukee, WI), an auxin influx transport inhibitor. To determine root lengths, primary roots grown in the above-mentioned supplemented media were stretched by forceps and photographed 13 d after

sowing. Statistical analysis of the data was performed with the SPSS version 7.5 software package (Statistical Products & Service Solutions, Chicago), and plots were obtained with the SigmaPlot 2000 version 6.0 program (Statistical Products & Service Solutions).

Hormone-Induced Gene Expression Analyses

Plants grown on agar plates as described above were collected 20 d after sowing and transferred to flasks containing 50 mL of one-half-strength Murashige and Skoog (no. M 0221, Duchefa Biochemie B.V., Haarlem, The Netherlands) liquid medium, which were incubated for 24 h at 225 rpm, 20°C ± 1°C, and 60% to 70% relative humidity under continuous illumination of 7,000 luxes. Ethanol solutions of 2,4-D or 24-epibrassinolide were then added to the liquid cultures to reach a final concentration of 50 or 100 nM, respectively. After incubation for 12 h in the same conditions, plants were immediately frozen in liquid nitrogen and stored at −80°C. RNA was extracted from frozen samples of 50 to 100 mg, using the Qiagen RNeasy Plant Mini Kit (no. 74904, Qiagen USA, Valencia, CA), following the instructions of the manufacturer. The eluate was incubated for 30 min at 37°C with 40 units of DNaseI. After inactivation of DNaseI at 70°C for 15 min, RNA was ethanol precipitated and resuspended in 40 μL of RNase-free water. About 4 μg of the RNA extracted from each sample was reverse transcribed using the SuperScript II RNase H RT following the instructions of the manufacturer (no. 18064-022, Invitrogen, Carlsbad, CA). The cDNA solution obtained in this way was diluted by adding 60 μL of distilled water.

Real-Time Quantitative PCR

Reaction mixes of 25 μL were prepared including 12.5 μL of the SYBR Green PCR Master Kit (no. 4309155, Applied Biosystems, Foster City, CA) containing the AmpliTaq Gold polymerase, 0.4 pmol of a primer pair, and 1 μL of cDNA. PCR amplifications were carried out in 96-well optical reaction plates on the ABI PRISM 7000 Sequence Detection System (Applied Biosystems). Three independent amplifications were performed from each cDNA sample. The thermal cycling program started with a step of 2 min at 50°C and 10 min at 95°C to activate the polymerase, followed by 40 cycles of 15 s at 95°C and 1 min at 60°C. Dissociation kinetics analyses of the amplification products were performed to check their specificity. Only the expected products were found to be amplified. The primer pairs used and the sizes of the expected amplification products are shown in Table IV. One of the primers of each pair contained the sequences of the ends of two contiguous exons to avoid amplification of genomic DNA.

Relative quantitation of gene expression was carried out using the $2^{-\Delta\Delta C_T}$ method (Livak and Schmittgen, 2001). Expression levels of the target genes were normalized using the C_T values obtained for the *OTC* (*ORNITINE TRANSCARBAMILASE*) housekeeping gene (Quesada et al., 1999), which was used as an endogenous reference. The relative amount of target gene transcripts was calculated as the difference in C_Ts for the target gene products and the reference gene products, given by $2^{-\Delta\Delta C_T}$, where $\Delta\Delta C_T$ was calculated as: $(C_{T, \text{target gene}} - C_{T, \text{reference gene}})_{\text{mutant}} - (C_{T, \text{target gene}} - C_{T, \text{reference gene}})_{\text{wild type}}$, in noninductive conditions; or $(C_{T, \text{target gene}} - C_{T, \text{reference gene}})_{\text{induced}} - (C_{T, \text{target gene}} - C_{T, \text{reference gene}})_{\text{noninduced}}$, in supplemented media. Confidence intervals were obtained by evaluating the expressions $2^{-(\Delta\Delta C_T + \text{SD})}$ and $2^{(\Delta\Delta C_T + \text{SD})}$, where SD is the SD of the $\Delta\Delta C_T$ value. Data were represented in Figure 6 as the relative gene expression normalized to an internal reference (*OTC*) and relative to gene expression in noninductive conditions in the wild type.

Positional Cloning

Low-resolution gene mapping was performed by using SSLP (Bell and Ecker, 1994) and cleaved-amplified polymorphic sequence (Konieczny and Ausubel, 1993) markers. Homozygous *ucu2-1* plants were crossed to Col-0, and *ucu2-2* and *ucu2-3* homozygotes were crossed to L*er*. Phenotypically mutant F_2 individuals were collected and frozen to extract their DNA as described by Ponce et al. (1999). Multiplex PCR amplification conditions and automated fragment sizing of amplified microsatellites were as described by Ponce et al. (1999). Map distances were determined using Kosambi's map function (Kosambi, 1944). Novel SSLP markers developed in this work are described in Table V.

Sequencing reactions were carried out on PCR amplification products, previously purified by ethanol precipitation, using ABI PRISM BigDye Terminator Cycle Sequencing version 2.0 Ready Reaction kits (Applied Biosystems) according to the instructions provided by the manufacturer, in a reaction volume of 5 μL, and GeneAmp PCR System 2400 (Applied Biosystems) thermal cycler. Sequencing electrophoresis and detection were performed on an ABI PRISM 3100 Genetic Analyzer (Applied Biosystems).

The sequences obtained were assembled with the Multiple Alignment Construction & Analysis Workbench program (version 2.0.5, Greg Schuler, National Center for Biotechnology Information, 1995). Sequences with homology to that of the *UCU2* gene were identified in the GenBank database (Benson et al., 2002; http://www.ncbi.nlm.nih.gov/) using the BLAST program (Altschul et al., 1997). Analyses of amino acid sequences were undertaken by using the tools available at the PROSITE database (Falquet et al., 2002; http://www.expasy.org/prosite/).

Southern-Blot Analysis

Genomic DNA was isolated from whole rosette leaves as previously reported (Dellaporta et al., 1983). Five micrograms of DNA was digested with *Sac*I or *Acc*I and electrophoresed (15 h at 30 V in a 0.8% [w/v] agarose gel in 0.5× Tris-borate/EDTA buffer) and then treated with depurination (no. N1907, Sigma), denaturation (no. N1531, Sigma), and neutralization (no. N1532, Sigma) solutions following the protocol provided by the manufacturer. Transference to a Hybond N$^+$ membrane (Amersham, Buckinghamshire, UK) was performed overnight in 2× SSC buffer (no. S6639, Sigma). Before prehybridization, the membrane was oven dried (10 min at 80°C) and cross linked (15 s under 70,000 μJ cm^{-2}). Prehybridization (1 h at 46°C) and hybridization (18 h at 46°C) were carried out in 20 and 30 mL, respectively, of a water solution of DIG Easy Hyb Granules (no. 1,796,895, Boehringer Mannheim/Roche, Basel), prepared as indicated by the manufacturer, in a hybridization oven. The membrane was hybridized with 30 ng mL^{-1} denatured (10 min at 95°C) digoxigenin 11-dUTP (no. 1,570,552, Boehringer Mannheim/Roche) probe, which had been synthesized as previously described (Ponce et al., 1998). The primers used to PCR synthesize the probes were the following: SeqMIL23.13F (5′-TCCTGAAGACAGTCTCAGTTC-3′) and SeqMIL23.10R (5′-CAGGTTGACATGATGTACACGC-3′) for probe 1, and SeqMIL23.11F (5′-GTCAGCTATAGAAAGATCTGAGC-3′) and SeqMIL23.11R (5′-AGCCTTCTCGATGGTTTGGTC-3′) for probe 2. Washes and detection were performed using the DIG Wash and Block buffer set (no. 1,585,762, Boehringer Mannheim/Roche) as indicated by the manufacturer. Detection was performed with anti-DIG-AP Fab fragments (no. 1,093,274, Boehringer Mannheim/Roche) and the chemiluminiscent phosphatase CDP-*Star* substrate (no. 1,685,627, Boehringer Mannheim/Roche). Autoradiograms were obtained on Hyperfilm ECL (Amersham-Pharmacia Biotech, Uppsala) exposed for about 2 h. Membranes were reprobed after being washed with water to remove the substrate and incubated twice in 0.3 M NaOH and 0.1% (w/v) SDS for 20 min at 37°C and rinsed in 2× SSC buffer to remove the probe.

Functional Complementation

To clone candidate genes in the pART7 vector (Gleave, 1992), the following oligonucleotides were designed. All had a 5′ tail (shown in lowercase), including restriction sites for *Kpn*I or *Xba*I (in bold): ClonMIL23.10F, 5′-gcc**ggtacc**TCTTCGTGAGTGACTTCGACG-3′; and ClonMIL23.4R, The ClonMIL23.10F and ClonMIL23.4R primers flanked a 2,441-bp fragment of the *At3g21640* gene that contains its whole open reading frame. The PCR product obtained was digested with *Kpn*I and *Xba*I and cloned into the pART7 vector (Gleave, 1992). Competent *Escherichia coli* DH5α cells were transformed, and the transformants were isolated on Luria-Bertani broth plates supplemented with 100 μg mL^{-1} ampicillin and later tested by PCR amplification for the presence of the transgene. Plasmid DNA was isolated and digested with *Not*I, and the restriction fragments were cloned into the pART27 vector in DH5α cells. Positive clones were selected on Luria-Bertani broth agar plates supplemented with 25 μg mL^{-1} streptomycin, 5% (w/v) X-Gal, and 50 mg mL^{-1} isopropylthio-β-galactoside, and tested by PCR for the presence of the construct. Plasmid DNA was isolated from these clones and used to transform chemical competent *Agrobacterium tumefaciens* C58C1 cells. Transformant *A. tumefaciens* cells were selected as described above and used to obtain liquid cultures that were used for in planta transformations

of Arabidopsis wild-type and mutant plants (Bechtold and Pelletier, 1998). The T_2 seeds obtained were sown in agar plates supplemented with 50 μg mL^{-1} kanamycin. PCR amplifications using primers flanking the *At3g21640* transcription unit were performed to confirm the presence of the transgene in the kanamycin-resistant T_2 plants.

Gene Expression Analysis

To determine whether or not the expression of candidate genes was affected in the *ucu2* mutants, RT-PCR amplifications of RNA extracted from leaves and flower buds were performed as described by Ponce et al. (2000). The primer pairs used corresponded to the 5′ region (SeqMIL23.10F, 5′-TCTT-CGTGAGTGACTTCGACG-3′; and SeqMIL23.2R, 5′-CTCTTGAGATGGCT-CACTATG-3′) or the 3′ region (SeqMIL23.4F, 5′-GAAGCAATTGGTCACT-GCAAC-3′; and SeqMIL23.4R, 5′-GGTAGATCTTTCACGTTGGTC-3′) of the *At3g21640* gene. Only the SeqMIL23.4F and SeqMIL23.4R primer pair was found useful for distinguishing between wild-type and *ucu2-3* sequences.

LITERATURE CITED

Abel S, Nguyen MD, Theologis A (1995) The PS-IAA4/5-like family of early auxin-inducible mRNAs in *Arabidopsis thaliana*. J Mol Biol **251:** 533–549

Altmann T (1999) Molecular physiology of brassinosteroids revealed by the analysis of mutants. Planta **208:** 1–11

Altmann T (2001) Brassinosteroid signaling in plants. Trends Endocrinol Metab **12:** 398–402

Altschul SF, Madden TL, Schäffer AA, Zhang JZ, Miller W, Lipman DJ (1997) Gapped BLAST and PSI-BLAST: a new generation of protein database search programs. Nucleic Acids Res **25:** 3389–3402

Bachmair A, Becker F, Masterson RV, Schell J (1990) Perturbation of the ubiquitin system causes leaf curling, vascular tissue alterations and necrotic lesions in a higher plant. EMBO J **9:** 4543–4549

Bancos S, Nomura T, Sato T, Molnar G, Bishop GJ, Koncz C, Yokota T, Nagy F, Szekeres M (2002) Regulation of transcript levels of the *Arabidopsis* cytochrome p450 genes involved in brassinosteroid biosynthesis. Plant Physiol **130:** 504–513

Barker N, Morin PJ, Clevers H (2000) The Yin-Yang of TCF/beta-catenin signaling. Adv Cancer Res **77:** 1–24

Bechtold N, Pelletier G (1998) *In planta Agrobacterium*-mediated transformation of adult *Arabidopsis thaliana* plants by vacuum infiltration. Methods Mol Biol **82:** 259–266

Bell CJ, Ecker JR (1994) Assignment of 30 microsatellite loci to the linkage map of *Arabidopsis*. Genomics **19:** 137–144

Bennett MJ, Marchant A, Green HG, May ST, Ward SP, Millner PA, Walker AR, Schulz B, Feldmann KA (1996) *Arabidopsis AUX1* gene: a permease-like regulator of root gravitropism. Science **273:** 948–950

Benson DA, Karsch-Mizrachi I, Lipman DJ, Ostell J, Rapp BA, Wheeler DL (2002) GenBank. Nucleic Acids Res **30:** 17–20

Berná G, Robles P, Micol JL (1999) A mutational analysis of leaf morphogenesis in *Arabidopsis thaliana*. Genetics **152:** 729–742

Bishop GJ, Koncz C (2002) Brassinosteroids and plant steroid hormone signaling. Plant Cell **14:** S97–S110

Bishop GJ, Yokota T (2001) Plants steroid hormones, brassinosteroids: current highlights of molecular aspects on their synthesis/metabolism, transport, perception and response. Plant Cell Physiol **42:** 114–120

Blatch GL, Lassle M (1999) The tetratricopeptide repeat: a structural motif mediating protein-protein interactions. Bioessays **21:** 932–939

Candela H, Martínez-Laborda A, Micol JL (1999) Venation pattern formation in *Arabidopsis thaliana* vegetative leaves. Dev Biol **205:** 205–216

Capdevila J, Izpisúa-Belmonte JC (2001) Patterning mechanisms controlling vertebrate limb development. Annu Rev Cell Dev Biol **17:** 87–132

Carland FM, McHale NA (1996) *LOP1*: a gene involved in auxin transport and vascular patterning in *Arabidopsis*. Development **122:** 1811–1819

Catterou M, Dubois F, Schaller H, Aubanelle L, Vilcot B, Sangwan-Norreel BS, Sangwan RS (2001) Brassinosteroids, microtubules and cell elongation in *Arabidopsis thaliana*: II. Effects of brassinosteroids on microtubules and cell elongation in the *bul1* mutant. Planta **212:** 673–683

Clouse S (2002) Brassinosteroid signaling: novel downstream components emerge. Curr Biol **12:** R485–R487

Cnops G, Wang X, Linstead P, Van Montagu M, Van Lijsebettens M, Dolan L (2000) *Tornado1* and *tornado2* are required for the specification of radial and circumferential pattern in the *Arabidopsis* root. Development **127:** 3385–3394

Cohen P, Frame S (2001) The renaissance of GSK3. Nat Rev Mol Cell Biol **2:** 769–776

Dellaporta SL, Wood J, Hicks JB (1983) A plant DNA minipreparation: version II. Plant Mol Biol Rep **4:** 19–21

Ephritikhine G, Fellner M, Vannini C, Lapous D, Barbier-Brygoo H (1999a) The *sax1* dwarf mutant of *Arabidopsis thaliana* shows altered sensitivity of growth responses to abscisic acid, auxin, gibberellins and ethylene and is partially rescued by exogenous brassinosteroid. Plant J **18:** 303–314

Ephritikhine G, Pagant S, Fujioka S, Takatsuto S, Lapous D, Caboche M, Kendrick RE, Barbier-Brygoo H (1999b) The *sax1* mutation defines a new locus involved in the brassinosteroid biosynthesis pathway in *Arabidopsis thaliana*. Plant J **18:** 315–320

Falquet L, Pagni M, Bucher P, Hulo N, Sigrist CJ, Hofmann K, Bairoch A (2002) THE PROSITE database, its status in 2002. Nucleic Acids Res **30:** 235–238

Faure JD, Vittorioso P, Santoni V, Fraisier V, Prinsen E, Barlier I, Van Onckelen H, Caboche M, Bellini C (1998) The *PASTICCINO* genes of *Arabidopsis thaliana* are involved in the control of cell division and differentiation. Development **125:** 909–918

Friedrichsen D, Chory J (2001) Steroid signaling in plants: from the cell surface to the nucleus. Bioessays **23:** 1028–1036

Friedrichsen DM, Joazeiro CA, Li J, Hunter T, Chory J (2000) Brassinosteroid-insensitive-1 is a ubiquitously expressed leucine-rich repeat receptor serine/threonine kinase. Plant Physiol **123:** 1247–1256

Friedrichsen DM, Nemhauser J, Muramitsu T, Maloof JN, Alonso J, Ecker JR, Furuya M, Chory J (2002) Three redundant brassinosteroid early response genes encode putative bHLH transcription factors required for normal growth. Genetics **162:** 1445–1456

Fujita H, Syono K (1996) Genetic analysis of the effects of polar auxin transport inhibitors on root growth in *Arabidopsis thaliana*. Plant Cell Physiol **37:** 1094–1101

Furutani I, Watanabe Y, Prieto R, Masukawa M, Suzuki K, Naoi K, Thitamadee S, Shikanai T, Hashimoto T (2000) The *SPIRAL* genes are required for directional control of cell elongation in *Arabidopsis thaliana*. Development **127:** 4443–4453

Gaedeke N, Klein M, Kolukisaoglu U, Forestier C, Muller A, Ansorge M, Becker D, Mamnun Y, Kuchler K, Schulz B et al. (2001) The *Arabidopsis thaliana* ABC transporter AtMRP5 controls root development and stomata movement. EMBO J **20:** 1875–1887

Galat A (2000) Sequence diversification of the FK506-binding proteins in several different genomes. Eur J Biochem **267:** 4945–4959

Galigniana MD, Radanyi C, Renoir JM, Housley PR, Pratt WB (2001) Evidence that the peptidylprolyl isomerase domain of the hsp90-binding immunophilin FKBP52 is involved in both dynein interaction and glucocorticoid receptor movement to the nucleus. J Biol Chem **276:** 14884–14889

Gleave AP (1992) A versatile binary vector system with a T-DNA organisational structure conducive to efficient integration of cloned DNA into the plant genome. Plant Mol Biol **20:** 1203–1207

Harrar Y, Bellini C, Faure JD (2001) FKBPs: at the crossroads of folding and transduction. Trends Plant Sci **6:** 426–431

Harrell JM, Kurek I, Breiman A, Radanyi C, Renoir JM, Pratt WB, Galigniana MD (2002) All of the protein interactions that link steroid receptor-hsp90-immunophilin heterocomplexes to cytoplasmic dynein are common to plant and animal cells. Biochemistry **41:** 5581–5587

Hashimoto T (2002) Molecular genetic analysis of left-right handedness in plants. Philos Trans R Soc Lond B Biol Sci **357:** 799–808

He JX, Gendron JM, Yang Y, Li J, Wang ZY (2002) The GSK3-like kinase BIN2 phosphorylates and destabilizes BZR1, a positive regulator of the brassinosteroid signaling pathway in *Arabidopsis*. Proc Natl Acad Sci USA **99:** 10185–10190

He Z, Wang ZY, Li J, Zhu Q, Lamb C, Ronald P, Chory J (2000) Perception of brassinosteroids by the extracellular domain of the receptor kinase BRI1. Science **288:** 2360–2363

Hemenway CS, Heitman J (1996) Immunosuppressant target protein FKBP12 is required for P-glycoprotein function in yeast. J Biol Chem **271:** 18527–18534

Kamphausen T, Fanghanel J, Neumann D, Schulz B, Rahfeld JU (2002) Characterization of *Arabidopsis thaliana* AtFKBP42 that is membrane-bound and interacts with Hsp90. Plant J **32:** 263–276

Kim GT, Tsukaya H, Uchimiya H (1998) The *ROTUNDIFOLIA3* gene of *Arabidopsis thaliana* encodes a new member of the cytochrome P-450 family that is required for the regulated polar elongation of leaf cells. Genes Dev **12:** 2381–2391

Kim L, Kimmel AR (2000) GSK3, a master switch regulating cell-fate specification and tumorigenesis. Curr Opin Genet Dev **10:** 508–514

Klimyuk VI, Jones JD (1997) *AtDMC1*, the *Arabidopsis* homologue of the yeast *DMC1* gene: characterization, transposon-induced allelic variation and meiosis-associated expression. Plant J **11:** 1–14

Koizumi K, Sugiyama M, Fukuda H (2000) A series of novel mutants of *Arabidopsis thaliana* that are defective in the formation of continuous vascular network: calling the auxin signal flow canalization hypothesis into question. Development **127:** 3197–3204

Koka CV, Cerny RE, Gardner RG, Noguchi T, Fujioka S, Takatsuto S, Yoshida S, Clouse SD (2000) A putative role for the tomato genes *DUMPY* and *CURL-3* in brassinosteroid biosynthesis and response. Plant Physiol **122:** 85–98

Konieczny A, Ausubel FM (1993) A procedure for mapping *Arabidopsis* mutations using co-dominant ecotype-specific PCR-based markers. Plant J **4:** 403–410

Kosambi DD (1944) The estimation of map distance from recombination values. Ann Eugen **12:** 172–175

Leyser HM, Lincoln CA, Timpte C, Lammer D, Turner J, Estelle M (1993) *Arabidopsis* auxin-resistance gene *AXR1* encodes a protein related to ubiquitin-activating enzyme E1. Nature **364:** 161–164

Li J, Chory J (1997) A putative leucine-rich repeat receptor kinase involved in brassinosteroid signal transduction. Cell **90:** 929–938

Li J, Chory J (1999) Brassinosteroid actions in plants. J Exp Bot **50:** 275–282

Li J, Nagpal P, Vitart V, McMorris TC, Chory J (1996) A role for brassinosteroids in light-dependent development of *Arabidopsis*. Science **272:** 398–401

Li J, Nam KH (2002) Regulation of brassinosteroid signaling by a GSK3/SHAGGY-like kinase. Science **295:** 1299–1301

Li J, Nam KH, Vafeados D, Chory J (2001a) BIN2, a new brassinosteroid-insensitive locus in *Arabidopsis*. Plant Physiol **127:** 14–22

Li J, Wen J, Lease KA, Doke JT, Tax FE, Walker JC (2002) BAK1, an *Arabidopsis* LRR receptor-like protein kinase, interacts with BRI1 and modulates brassinosteroid signaling. Cell **110:** 213–222

Li X, Yost HJ, Virshup DM, Seeling JM (2001b) Protein phosphatase 2A and its B56 regulatory subunit inhibit Wnt signaling in *Xenopus*. EMBO J **20:** 4122–4131

Liscum E, Reed JW (2002) Genetics of Aux/IAA and ARF action in plant growth and development. Plant Mol Biol **49:** 387–400

Livak KJ, Schmittgen TD (2001) Analysis of relative gene expression data using real-time quantitative PCR and the 2(-Delta Delta C(T)) Method. Methods **25:** 402–408

Luschnig C (2002) Auxin transport: ABC proteins join the club. Trends Plant Sci **7:** 329

Marchant A, Kargul J, May ST, Muller P, Delbarre A, Perrot-Rechenmann C, Bennett MJ (1999) AUX1 regulates root gravitropism in *Arabidopsis* by facilitating auxin uptake within root apical tissues. EMBO J **18:** 2066–2073

Mathur J, Molnar G, Fujioka S, Takatsuto S, Sakurai A, Yokota T, Adam G, Voigt B, Nagy F, Maas C et al. (1998) Transcription of the *Arabidopsis* *CPD* gene, encoding a steroidogenic cytochrome P450, is negatively controlled by brassinosteroids. Plant J **14:** 593–602

Mattsson J, Sung ZR, Berleth T (1999) Responses of plant vascular systems to auxin transport inhibition. Development **126:** 2979–2991

Meinke D, Koornneef M (1997) Community standards for *Arabidopsis* genetics. Plant J **12:** 247–253

Müssig C, Fischer S, Altmann T (2002) Brassinosteroid-regulated gene expression. Plant Physiol **129:** 1241–1251

Nagpal P, Walker LM, Young JC, Sonawala A, Timpte C, Estelle M, Reed JW (2000) *AXR2* encodes a member of the Aux/IAA protein family. Plant Physiol **123:** 563–574

Nakaya M, Tsukaya H, Murakami N, Kato M (2002) Brassinosteroids control the proliferation of leaf cells of *Arabidopsis thaliana*. Plant Cell Physiol **43:** 239–244

Noh B, Murphy AS, Spalding EP (2001) Multidrug resistance-like genes of *Arabidopsis* required for auxin transport and auxin-mediated development. Plant Cell **13:** 2441–2454

Nomura T, Nakayama M, Reid JB, Takeuchi Y, Yokota T (1997) Blockage of brassinosteroid biosynthesis and sensitivity causes dwarfism in garden pea. Plant Phisiol **113:** 31–37

Owens-Grillo JK, Stancato LF, Hoffmann K, Pratt WB, Krishna P (1996) Binding of immunophilins to the 90 kDa heat shock protein (hsp90) via a tetratricopeptide repeat domain is a conserved protein interaction in plants. Biochemistry **35:** 15249–15255

Parry G, Delbarre A, Marchant A, Swarup R, Napier R, Perrot-Rechenmann C, Bennett MJ (2001) Novel auxin transport inhibitors phenocopy the auxin influx carrier mutation aux1. Plant J **25:** 399–406

Pérez-Pérez JM, Ponce MR, Micol JL (2002) The *UCU1 Arabidopsis* gene encodes a SHAGGY/GSK3-like kinase required for cell expansion along the proximodistal axis. Dev Biol **242:** 161–173

Ponce MR, Pérez-Pérez JM, Piqueras P, Micol JL (2000) A multiplex reverse transcriptase-polymerase chain reaction method for fluorescence-based semiautomated detection of gene expression in *Arabidopsis thaliana*. Planta **211:** 606–608

Ponce MR, Quesada V, Micol JL (1998) Rapid discrimination of sequences flanking and within T-DNA insertions in the *Arabidopsis* genome. Plant J **14:** 497–501

Ponce MR, Robles P, Micol JL (1999) High-throughput genetic mapping in *Arabidopsis thaliana*. Mol Gen Genet **261:** 408–415

Pratt WB, Krishna P, Olsen LJ (2001) Hsp90-binding immunophilins in plants: the protein movers. Trends Plant Sci **6:** 54–58

Quesada V, Ponce MR, Micol JL (1999) *OTC* and *AUL1*, two convergent and overlapping genes in the nuclear genome of *Arabidopsis thaliana*. FEBS Lett **461:** 101–106

Rédei GP (1962) Supervital mutants of *Arabidopsis*. Genetics **47:** 443–460

Richter K, Buchner J (2001) Hsp90: chaperoning signal transduction. J Cell Physiol **188:** 281–290

Robles P, Micol JL (2001) Genome-wide linkage analysis of *Arabidopsis* genes required for leaf development. Mol Genet Genomics **266:** 12–19

Schiene-Fischer C, Yu C (2001) Receptor accessory folding helper enzymes: the functional role of peptidyl prolyl cis/trans isomerases. FEBS Lett **495:** 1–6

Seeling JM, Miller JR, Gil R, Moon RT, White R, Virshup DM (1999) Regulation of beta-catenin signaling by the B56 subunit of protein phosphatase 2A. Science **283:** 2089–2091

Semiarti E, Ueno Y, Tsukaya H, Iwakawa H, Machida C, Machida Y (2001) The *ASYMMETRIC LEAVES2* gene of *Arabidopsis thaliana* regulates formation of a symmetric lamina, establishment of venation and repression of meristem-related homeobox genes in leaves. Development **128:** 1771–1783

Serrano-Cartagena J, Candela H, Robles P, Ponce MR, Pérez-Pérez JM, Piqueras P, Micol JL (2000) Genetic analysis of *incurvata* mutants reveals three independent genetic operations at work in *Arabidopsis* leaf morphogenesis. Genetics **156:** 1363–1377

Serrano-Cartagena J, Robles P, Ponce MR, Micol JL (1999) Genetic analysis of leaf form mutants from the *Arabidopsis* Information Service collection. Mol Gen Genet **261:** 725–739

Sieberer T, Seifert GJ, Hauser MT, Grisafi P, Fink GR, Luschnig C (2000) Post-transcriptional control of the *Arabidopsis* auxin efflux carrier EIR1 requires AXR1. Curr Biol **10:** 1595–1598

Sieburth LE (1999) Auxin is required for leaf vein pattern in *Arabidopsis*. Plant Physiol **121:** 1179–1190

Szekeres M, Nemeth K, Koncz-Kalman Z, Mathur J, Kauschmann A, Altmann T, Redei GP, Nagy F, Schell J, Koncz C (1996) Brassinosteroids rescue the deficiency of CYP90, a cytochrome P450, controlling cell elongation and de-etiolation in *Arabidopsis*. Cell **85:** 171–182

Takahashi T, Gasch A, Nishizawa N, Chua NH (1995) The *DIMINUTO* gene of *Arabidopsis* is involved in regulating cell elongation. Genes Dev **9:** 97–107

Terol J, Bargues M, Carrasco P, Pérez-Alonso M, Paricio N (2002) Molecular characterization and evolution of the protein phosphatase 2A B′ regulatory subunit family in plants. Plant Physiol **129:** 808–822

Thitamadee S, Tuchihara K, Hashimoto T (2002) Microtubule basis for left-handed helical growth in *Arabidopsis*. Nature **417:** 193–196

Tsiantis M, Brown MI, Skibinski G, Langdale JA (1999) Disruption of auxin transport is associated with aberrant leaf development in maize. Plant Physiol **121:** 1163–1168

Tsiantis M, Langdale J (1998) The formation of leaves. Curr Opin Plant Biol **1:** 43–48

Ueda K, Okamura N, Hirai M, Tanigawara Y, Saeki T, Kioka N, Komano T, Hori R (1992) Human P-glycoprotein transports cortisol, aldosterone, and dexamethasone, but not progesterone. J Biol Chem **267:** 24248–24252

Vittorioso P, Cowling R, Faure JD, Caboche M, Bellini C (1998) Mutation in the *Arabidopsis PASTICCINO1* gene, which encodes a new FK506-binding protein-like protein, has a dramatic effect on plant development. Mol Cell Biol **18:** 3034–3043

Vucich VA, Gasser CS (1996) Novel structure of a high molecular weight FK506 binding protein from *Arabidopsis thaliana*. Mol Gen Genet **252:** 510–517

Wang ZY, Nakano T, Gendron J, He J, Chen M, Vafeados D, Yang Y, Fujioka S, Yoshida S, Asami T et al. (2002) Nuclear-localized BZR1 mediates brassinosteroid-induced growth and feedback suppression of brassinosteroid biosynthesis. Dev Cell **2:** 505–513

Wang ZY, Seto H, Fujioka S, Yoshida S, Chory J (2001) BRI1 is a critical component of a plasma-membrane receptor for plant steroids. Nature **410:** 380–383

Wilson AK, Pickett FB, Turner JC, Estelle M (1990) A dominant mutation in *Arabidopsis* confers resistance to auxin, ethylene and abscisic acid. Mol Gen Genet **222:** 377–383

Xiong L, Lee H, Ishitani M, Zhu JK (2002) Regulation of osmotic stress-responsive gene expression by the *LOS6/ABA1* locus in *Arabidopsis*. J Biol Chem **277:** 8588–8596

Yin Y, Wang ZY, Mora-García S, Li J, Yoshida S, Asami T, Chory J (2002) BES1 accumulates in the nucleus in response to brassinosteroids to regulate gene expression and promote stem elongation. Cell **109:** 181–191

Young JC, Obermann WM, Hartl FU (1998) Specific binding of tetratricopeptide repeat proteins to the C-terminal 12-kDa domain of hsp90. J Biol Chem **273:** 18007–18010